

Casimir Forces between Spherical Particles in a Critical Fluid and Conformal Invariance

E. Eisenriegler¹ and U. Ritschel²

¹*Institut für Festkörperforschung, Forschungszentrum Jülich, 52425 Jülich (FR Germany)*

²*Fachbereich Physik, Universität GH Essen, 45117 Essen (FR Germany)*

Abstract

Mesoscopic particles immersed in a critical fluid experience long-range Casimir forces due to critical fluctuations. Using field theoretical methods, we investigate the Casimir interaction between two spherical particles and between a single particle and a planar boundary of the fluid. We exploit the conformal symmetry at the critical point to map both cases onto a highly symmetric geometry where the fluid is bounded by two *concentric* spheres with radii R_- and R_+ . In this geometry the singular part of the free energy \mathcal{F} only depends upon the ratio R_-/R_+ , and the stress tensor, which we use to calculate \mathcal{F} , has a particularly simple form. Different boundary conditions (surface universality classes) are considered, which either break or preserve the order-parameter symmetry. We also consider profiles of thermodynamic densities in the presence of two spheres. Explicit results are presented for an ordinary critical point to leading order in $\epsilon = 4 - d$ and, in the case of preserved symmetry, for the Gaussian model in arbitrary spatial dimension d . Fundamental short-distance properties, such as profile behavior near a surface or the behavior if a sphere has a ‘small’ radius, are discussed and verified. The relevance for colloidal solutions is pointed out.

PACS numbers: 05.70.Jk, 68.35.Rh, 75.40.Cx, 75.30.Pd, 82.70.Dd

Typeset using REVTeX

I. INTRODUCTION

Consider a fluid system close to a critical point, for example a fluid near the liquid-gas critical point, a binary liquid near the consolute point, or liquid ^4He near the λ -point. Due to the long correlation length a local perturbation, as provided by the wall of the container or by the surfaces of immersed colloid particles, is not screened within a few atomic layers but influences the system over appreciable distances. This gives rise to a long-range interaction between immersed particles or a particle and a wall, as pointed out by Fisher and de Gennes [1,2]. The forces may be termed critical Casimir forces [3] on account of the close formal relationship with the usual Casimir forces [4] due to quantum fluctuations of the electromagnetic field. An interesting feature of the critical Casimir effect is that it can be turned on and off by changing the magnitude of the correlation length, e.g. by changing the temperature.

The simplest and most-considered geometry for the critical (as well as the electromagnetic) Casimir effect is the parallel-plate geometry. Results have been obtained in spatial dimensions $d = 2$ by using conformal invariance [5–9] and in $d = 4 - \epsilon$ [10–13]. In this paper we consider *spherical boundary surfaces*, i.e. spheres immersed in a critical fluid. Many of the general model-independent properties for this geometry are also discussed in a recent letter by Burkhardt and one of the present authors [14].

The spherical shape is of immediate relevance for colloidal particles [15,16], and besides the planar boundary it is the simplest boundary shape for theoretical analyses. The reason is that systems right at the critical point display an invariance not only with respect to homogenous dilatations but also with respect to conformal or angle-preserving coordinate transformations [17]. The class of special conformal transformations [18] which exists in arbitrary spatial dimension d maps spheres onto spheres. This has been used to study the critical properties of an infinite system with a single spherical hole (particle) and of a finite system with a spherical boundary by conformally mapping results for the half-space [19,20].

An infinite system with *two* arbitrary non-overlapping spherical holes (particles) may be obtained by conformally mapping a highly symmetric finite system which is bounded by two concentric spheres [21]. This is shown in Fig. 1 and follows from the special conformal transformation

$$\frac{\mathbf{r}'}{r'^2} = \frac{\mathbf{r} + \mathbf{R}}{|\mathbf{r} + \mathbf{R}|^2} - \frac{\mathbf{R}}{2R^2} \quad (1.1)$$

which maps the sphere of radius R centered at the origin of \mathbf{r} -space onto a plane in \mathbf{r}' -space that is perpendicular to \mathbf{R} and passes through the origin. Two spheres with fixed radii R_- , R_+ centered about the origin of \mathbf{r} -space (and depicted in Fig. 1 a) map onto two spherical particles in \mathbf{r}' -space, as shown in Fig. 1 b. The points of intersection I, II, III, IV with the r'_\perp -axis have the coordinates

$$(r'_{\perp I}, r'_{\perp II}, r'_{\perp III}, r'_{\perp IV}) = 2R \left(-\frac{R_+ + R}{R_+ - R}, -\frac{R_+ - R}{R_+ + R}, \frac{R - R_-}{R + R_-}, \frac{R + R_-}{R - R_-} \right) \quad (1.2)$$

with $R_- < R < R_+$.

Two cases of particular interest will be studied in detail below:

- (i) For $R = \sqrt{R_- R_+}$, the *two spheres* in \mathbf{r}' -space have *equal size* (SES), since $r'_{\perp I} = -r'_{\perp IV}$ and $r'_{\perp II} = -r'_{\perp III}$.
- (ii) For $R \rightarrow R_+$, the left sphere reduces to a plane through the origin, which is denoted by a broken line in Fig. 1 b. This corresponds to *one sphere* with radius R_1 near a *planar wall* (SPW) of the container.

One may also consider a single spherical particle immersed in a critical fluid inside a *spherical container*. This geometry is obtained from the concentric geometry via (1.1) when R is chosen *outside* the interval (R_-, R_+) . For $R > R_+$ the order of the intersection points is II, III, IV, I, as in the concentric geometry of Fig. 1 a, and sphere a remains inside sphere b . For $0 < R < R_-$ the order is IV, I, II, III, and sphere a is located outside sphere b .

An important parameter of the two-sphere geometry is the *cross ratio* of intersection points, which remains invariant under conformal transformations [17,18]. Instead of working directly with the cross ratio, it is convenient to introduce the related invariant quantity

$$\kappa = 1 + 2 \frac{(r'_{\perp IV} - r'_{\perp I})(r'_{\perp III} - r'_{\perp II})}{(r'_{\perp IV} - r'_{\perp III})(r'_{\perp II} - r'_{\perp I})}, \quad (1.3)$$

which can be written as

$$\kappa = \frac{|s_{12}^2 - R_1^2 - R_2^2|}{2R_1R_2} \quad (1.4)$$

in either of the above geometries. Here R_1 and R_2 are the radii of spheres a and b , respectively, and s_{12} is the distance between their centers. On comparing with the concentric geometry of Fig. 1 a, where $s_{12} = 0$ and where R_1 and R_2 have been denoted by R_- and R_+ , respectively, one finds from (1.4)

$$\kappa = \frac{1}{2} \left(\rho + \rho^{-1} \right), \quad 1 < \kappa < \infty, \quad (1.5)$$

with

$$\rho = \frac{R_-}{R_+}, \quad 0 < \rho < 1. \quad (1.6)$$

One can also obtain (1.5) by inserting (1.2) into (1.3), which demonstrates the conformal invariance of κ since the parameter R of (1.1) drops out. It follows from (1.3) or (1.4) that $\kappa = 1$ corresponds to two particles that touch, while $\kappa \rightarrow \infty$ describes the situation where one or both of the radii R_1, R_2 are much smaller than the remaining lengths in the two-sphere configuration.

Now let us turn our attention to the free energy. For two non-overlapping spherical particles in an infinite critical medium we consider

$$\delta F(s_{12}, R_1, R_2) = F_{a,b}(s_{12}, R_1, R_2) - U_a(R_1) - U_b(R_2), \quad s_{12} \geq R_1 + R_2. \quad (1.7)$$

Here F is the singular part [22] of the free energy for immersing two particles into an infinitely extended fluid, while U is that for immersing a single particle. δF determines the Casimir force, $-\partial \delta F / \partial s_{12}$, and it vanishes as the separation s_{12} tends to infinity with

R_1, R_2 fixed. For the single particle (a, R_1) in the fluid with spherical confinement (b, R_2) one may consider a similar expression $\delta F(s_{12}, R_1, R_2)$ with $s_{12} + R_1 \leq R_2$, where $U_a(R_1)$ and $\bar{U}_b(R_2)$, the free energy of the spherical container without a particle, are subtracted from the total free energy. This expression vanishes as R_2 tends to infinity with R_1 and s_{12} fixed. Right at the bulk critical point the quantities δF are invariant under special conformal transformations [18,23] and can only depend on the conformal invariant κ in (1.4):

$$\delta F(s_{12}, R_1, R_2) = k_B T_c \mathcal{F}(\kappa) \quad (1.8)$$

It follows from the above arguments that δF for two particles in the infinite critical liquid and δF for the single particle in the spherically confined liquid both obey (1.8) with the same function $\mathcal{F}(\kappa)$. We note two special cases. First, for a single sphere with radius R_1 and with its closest point at a distance D from a planar wall (SPW), the Casimir interaction is

$$\delta F_{\text{SPW}}(D, R_1) = k_B T_c \mathcal{F}(1 + D/R_1) . \quad (1.9)$$

This follows from (1.8) by substituting $s_{12} = R_1 + R_2 + D$ and with $R_2 \rightarrow \infty$. Second, for the concentric geometry (CON) of Fig. 1 a, the result reads

$$\delta F_{\text{CON}}(R_-, R_+) = k_B T_c \mathcal{F}(\kappa(R_-/R_+)) , \quad (1.10)$$

with $\kappa(\rho)$ given by (1.5). Due to the high symmetry, the concentric geometry is especially convenient for the explicit evaluation of the universal scaling function $\mathcal{F}(\kappa)$.

The scaling function \mathcal{F} depends on both the bulk universality class [24] and the surface universality classes a, b [25,26] of the critical system. For a liquid-gas critical point or a critical consolute point of a binary mixture, a and b correspond to the Ising model with surface magnetic fields [25–28] either parallel (\uparrow, \uparrow) or antiparallel (\uparrow, \downarrow) depending on whether the two surfaces favor the same or different signs of the order parameter. Liquid ${}^4\text{He}$ at the λ -point belongs to the bulk universality class of the XY model, and surfaces are expected to suppress the superfluid order [29], corresponding to the surface universality class O of the ‘ordinary transition’ [25,26]. One may also consider tricritical bulk universality classes both for mixtures of ordinary liquids and of ${}^3\text{He}$ – ${}^4\text{He}$. It is also interesting to consider the multicritical surface universality class SB of the ‘special transition’ [25,26].

Exact results for \mathcal{F} have been obtained by Burkhardt and Eisenriegler [14] for the critical Ising model with pairs of surface universality classes $(a, b) = (O, O), (O, \uparrow), (\uparrow, \uparrow)$, and (\uparrow, \downarrow) in spatial dimension $d = 2$. In the present paper we investigate \mathcal{F} for d near the upper critical dimension $d_c = 4$. For the combinations $(a, b) = (\uparrow, \uparrow), (\uparrow, \downarrow), (\uparrow, O)$, and (\uparrow, SB) , where the order parameter symmetry is broken, the leading behavior in the ϵ -expansion follows from mean-field theory. This will be considered in Sec. III. Here we make close contact to the work of Indekeu et al. [11] for the parallel-plate geometry and of Gnuzmann and Ritschel [21] for the order-parameter profile in the concentric geometry for (\uparrow, \uparrow) . For the symmetry-preserving combinations $(O, O), (O, SB)$, and (SB, SB) , the leading behavior is that of the Gaussian model. Since the Gaussian model is conformally invariant for all $d > 2$, it is instructive to consider the above pairs of boundaries in general d . This is carried out in Sec. IV. The parallel-plate result (Krech and Dietrich [12]) emerges as a special case.

The explicit evaluation of the different universal scaling functions \mathcal{F} in Secs. III and IV are preceded in Sec. II by a discussion of general relationships involving \mathcal{F} which hold

for all spatial dimensions and universality classes of interest. We discuss the limits $\kappa \rightarrow 1$ and $\kappa \rightarrow \infty$, which have also been addressed in Ref. [14] and correspond to $\rho \rightarrow 1$ and $\rho \rightarrow 0$, respectively. For $\rho \rightarrow 1$, the scaling functions \mathcal{F} are determined by the amplitudes of the Casimir effect in *parallel-plate* geometry [5–13]. For $\rho \rightarrow 0$, we use the *small-sphere* expansion [14] (a kind of short-distance expansion) to relate \mathcal{F} to the amplitudes of the bulk correlation function and of the profile in the half-space of either the order parameter or the energy density, depending on the pair a, b of universality classes. We also discuss how \mathcal{F} can be conveniently calculated from the thermal average of the *stress tensor* [18]. Furthermore, we discuss the profiles of thermodynamic densities in the presence of two spheres [21]. For the particular case of a sphere and a planar wall (SPW), we use a short-distance expansion [30,31,13] to relate the behavior of the profile near the wall to the average of the stress tensor at the wall, i.e. to \mathcal{F} . All the general relationships are consistent with the explicit results in Secs. III and IV.

Sec. V contains our conclusions.

II. GENERAL RELATIONSHIPS

Here we discuss several important relationships which involve the scaling function \mathcal{F} of the free energy. They are of a general character and apply to most of the bulk and surface universality classes and spatial dimensions d which are of interest.

A. Free energy and the stress tensor

While conformal coordinate transformations of the two-sphere geometry preserve κ (and thus leave δF invariant), certain non-conformal transformations preserve the spherical shape of the boundaries but change κ . In equation (A2) we consider a transformation which increases the distance s_{12} of the two non-overlapping spheres of Fig. 1 b keeping R_1 and R_2 fixed. This is directly related to the Casimir force. In the concentric geometry of Fig. 1 a one may apply the infinitesimal transformation $\mathbf{r} \rightarrow \hat{\mathbf{r}}$ defined by

$$\hat{\mathbf{r}} - \mathbf{r} = \alpha \mathbf{r} \Theta(r - r_0) , \quad \alpha \ll 1 \quad (2.1)$$

which increases the radial component of \mathbf{r} by a fraction α if $r > r_0$. Choosing r_0 between R_- and R_+ , one sees that R_+ increases while R_- remains unchanged. Consequently, ρ and κ are changed. The effect of these transformations on δF can be written as an integral over the stress-energy tensor T_{kl} [18]. In the concentric case

$$\rho \frac{d}{d\rho} \delta F_{\text{CON}}(\rho) = k_B T_c S_d r_0^d \langle T_{nn}(r_0) \rangle_{\text{CON}} , \quad (2.2)$$

as we show in more detail in Appendix A. Here $S_d = 2\pi^{d/2}/\Gamma(d/2)$ is the surface area of the d -dimensional unit sphere, and $T_{nn}(r_0)$ is the radial component (normal to the spherical surfaces) of the stress tensor at a distance r_0 from the center. The thermal average at the right hand side of Eq. (2.2) is taken at the critical fixed point, where the trace of the stress tensor vanishes [18]. Since r_0 is arbitrary in the interval (R_-, R_+) ,

$$\langle T_{nn}(r_0) \rangle_{\text{CON}} = (2r_0)^{-d} Y(\rho) , \quad (2.3)$$

where we have included a factor 2^{-d} for convenience below. In evaluating $\mathcal{F}(\kappa)$ and the Casimir forces in Sec. III and IV, we have found it convenient to first calculate the scaling function Y defined in (2.3) and then integrate the result according to (2.2).

B. Free energy for $\kappa \rightarrow 1$

The limit $\rho \rightarrow 1$ corresponds to the parallel-plate geometry. The concentric geometry becomes equivalent to the parallel-plate geometry if we let $R_+ \rightarrow \infty$ while keeping the width $L = R_+ - R_-$ fixed. In this limit $1 - \rho = L/R_+$ tends to zero. With the usual notation [3,11,12] $\Delta_{a,b}/L^{d-1}$ for the Casimir free energy per $k_B T$ and surface area of one of the two parallel plates a, b ,

$$\delta F_{\text{CON}}(\rho) \rightarrow k_B T_c \Delta_{a,b} (1 - \rho)^{1-d} S_d \quad (2.4a)$$

and

$$Y(\rho) \rightarrow \Delta_{a,b} (d - 1) 2^d (1 - \rho)^{-d} \quad (2.4b)$$

as $\rho \rightarrow 1$. Eq. (2.4a) also determines the Casimir interaction of non-overlapping spheres that nearly touch. This follows from the form $S_d \Delta_{a,b} [2(\kappa - 1)]^{-(d-1)/2}$ of \mathcal{F} for $0 < \kappa - 1 \ll 1$ as implied by (1.10) and (1.5). In this geometry the limiting form reads [14]

$$\delta F(s_{12}, R_1, R_2) \rightarrow k_B T_c S_d \Delta_{a,b} \left[2(R_1^{-1} + R_2^{-1}) D \right]^{-(d-1)/2} . \quad (2.5)$$

Here (1.8) and (1.4) have been used, $D \equiv s_{12} - R_1 - R_2$ is the distance between the closest points of the two spherical surfaces (i.e. $r'_{\perp \text{III}} - r'_{\perp \text{II}}$ in Fig. 1b), and we assume $D \ll R_1, R_2$. In the limit $R_2^{-1} \rightarrow 0$, the right hand side of (2.5) determines the Casimir interaction $\delta F_{\text{SPW}}(D, R_1)$ of a single sphere close to a planar wall ($D \ll R_1$).

C. Small-sphere expansion and free energy for $\kappa \rightarrow \infty$

In the other limit $\rho \rightarrow 0$, where the radius of the inner sphere is much smaller than that of the outer boundary, one may use a short-distance expansion introduced in Ref. [14]. In this expansion the Boltzmann weight $\exp(-\mathcal{H}_S)$ which generates in the critical system a spherical hole S with center at \mathbf{r}_S and radius R_S is written in terms of local fluctuating quantities (operators) $\Xi(\mathbf{r}_S)$ and non-fluctuating amplitudes \mathcal{X} in the form

$$\frac{e^{-\mathcal{H}_S}}{\langle e^{-\mathcal{H}_S} \rangle_{\text{bulk}}} = 1 + \sigma \quad (2.6a)$$

with

$$\sigma = \sum_{\Xi} \mathcal{X}_{\Xi}(R_S) \Xi(\mathbf{r}_S) . \quad (2.6b)$$

The relation (2.6) holds in thermal averages or correlation functions containing other fluctuating quantities (operators) or boundaries [32] with distances from \mathbf{r}_S that are much larger than R_S . We mention a few examples where (2.6) is useful: Consider the thermal average $\langle \tilde{\Psi} \rangle_{S \text{ in bulk}}$ of a *primary* operator $\tilde{\Psi}(\mathbf{r})$ [33] such as the order parameter or the energy density in an infinite critical system (bulk) with a spherical hole S . By means of (2.6a) one finds

$$\langle \tilde{\Psi}(\mathbf{r}) \rangle_{S \text{ in bulk}} = \langle e^{-\mathcal{H}_S} \tilde{\Psi}(\mathbf{r}) \rangle_{\text{bulk}} / \langle e^{-\mathcal{H}_S} \rangle_{\text{bulk}} = \langle (1 + \sigma) \cdot \tilde{\Psi}(\mathbf{r}) \rangle_{\text{bulk}} \quad (2.7)$$

since the bulk average of σ vanishes. As another example consider the concentric geometry, which may be viewed as a critical system inside a full spherical container (fc) with Hamiltonian \mathcal{H}_{fc} , where a hole S is generated by adding \mathcal{H}_S . We are interested in the combination of free energies

$$(F_{S \text{ in fc}} - F_{\text{fc}}) - (F_{S \text{ in bulk}} - F_{\text{bulk}}) = k_B T_c \left[-\ln \langle e^{-\mathcal{H}_S} \rangle_{\text{fc}} + \ln \langle e^{-\mathcal{H}_S} \rangle_{\text{bulk}} \right] = -k_B T_c \ln \langle 1 + \sigma \rangle_{\text{fc}}, \quad (2.8)$$

the singular part of which is the function δF_{CON} in (1.10). As a third example one may use (2.6a) also to study the behavior of $\langle \tilde{\Psi}(\mathbf{r}) \rangle$ in the concentric geometry as $R_- \rightarrow 0$. One finds

$$\langle \tilde{\Psi}(\mathbf{r}) \rangle_{\text{CON}} - \langle \tilde{\Psi}(\mathbf{r}) \rangle_{\text{fc}} \longrightarrow \langle \sigma \tilde{\Psi}(\mathbf{r}) \rangle_{\text{fc}} - \langle \sigma \rangle_{\text{fc}} \langle \tilde{\Psi}(\mathbf{r}) \rangle_{\text{fc}} \quad (2.9)$$

to first order in σ . This relation also applies for $\tilde{\Psi} \rightarrow T_{nn}$, (see (2.3)). Further, the expansion (2.6b) holds also if the distant boundary is not a sphere concentric to S but, for example, a planar wall [34], and it should also apply slightly away from the critical point [35].

Which quantities Ξ appear in (2.6b) depends upon the universality class of the surface of S . In case of the surface universality classes O and SB that do not break the $O(N)$ symmetry of the N -component order parameter $\vec{\Phi}$ at the bulk critical point, all the Ξ 's are also $O(N)$ invariant, and the leading Ξ is the energy density $\vec{\Phi}^2$ [36]. For symmetry-breaking surfaces we only consider the case of a one-component order parameter Φ and the class \uparrow or \downarrow . In this case Ξ 's, which are odd and even under $\Phi \rightarrow -\Phi$ both appear in the expansion. The leading Ξ is the order parameter Φ and the leading even Ξ is the energy density.

In (2.6) R_S is assumed to be large on a microscopic scale. The amplitudes \mathcal{X} for $\Xi = \Phi$ or Φ^2 can be derived explicitly. They follow from the known result [19] for the profile $\langle \tilde{\Psi}(\mathbf{r}) \rangle_{S \text{ in bulk}}$ of the primary operators $\tilde{\Psi} = \Phi$ or Φ^2 by comparing with (2.7). From the leading behavior for $|r - r_S| \gg R_S$,

$$\mathcal{X}_\Psi = \frac{A_a^\Psi}{B_\Psi} (R_S)^{x_\Psi} \quad (2.10)$$

for $\Psi = \Phi$ or $\Psi = \Phi^2$, respectively [14]. Here a denotes the surface universality class of S , A is the amplitude in the critical profile

$$\langle \Psi(\mathbf{r}_\parallel, z) \rangle_{\text{half space}}^{(a)} = A_a^\Psi (2z)^{-x_\Psi} \quad (2.11)$$

of Ψ in a half-space with surface universality class a , and B is the amplitude of the bulk correlation function

$$\langle \Psi(\mathbf{r}) \Psi(0) \rangle_{\text{bulk}} = B_\Psi r^{-2x_\Psi}, \quad (2.12)$$

which also identifies x_Ψ as the bulk exponent of Ψ .

Now we may calculate δF_{CON} for small ρ as the singular part of (2.8) by using (2.6b) and (2.10), with the result

$$\delta F_{\text{CON}}(\rho)/k_B T_c \longrightarrow -\mathcal{X}_\Psi \cdot \langle \Psi(0) \rangle_{\text{fc}} = -\frac{A_a^\Psi A_b^\Psi}{B_\Psi} \rho^{x_\Psi}, \quad (2.13a)$$

where $\Psi = \Phi$ if both surfaces a, b are symmetry-breaking and $\Psi = \Phi^2$ if one or both preserve the symmetry of the order parameter. Here we have identified R_S with R_- of Fig. 1a and have used the fact that the profile $\langle \Psi(0) \rangle_{\text{fc}}$ at the center of a full spherical container with radius R_+ and surface universality class b is given by $A_b^\Psi (R_+)^{-x_\Psi}$ (see [19]). Below we will also need the small- ρ limit

$$Y(\rho) \rightarrow -2^d S_d^{-1} x_\Psi \rho^{x_\Psi} \frac{A_a^\Psi A_b^\Psi}{B_\Psi} \quad (2.13b)$$

of the stress-tensor scaling function defined in (2.3). This follows either from (2.13a) by means of (2.2) or by inserting (2.6b) and (2.10) into (2.9) with $\tilde{\Psi}(\mathbf{r}) \rightarrow T_{nn}(r_0)$ and using $\langle T_{kl} \rangle_{\text{fc}} = 0$ and [30]

$$\langle \Psi(0) T_{nn}(r_0) \rangle_{\text{fc}} = -r_0^{-d} (R_+)^{-x_\Psi} x_\Psi S_d^{-1} A_b^\Psi. \quad (2.14)$$

Eq. (2.13a) also implies, via (1.10) and (1.5), the form $-\left(A_a^\Psi A_b^\Psi / B_\Psi\right) (2\kappa)^{-x_\Psi}$ for the scaling function \mathcal{F} in (1.8) if $\kappa \gg 1$. This leads to the Casimir interaction [14]

$$\delta F(s_{12}, R_1, R_2) \rightarrow -k_B T_c \frac{A_a^\Psi A_b^\Psi}{B_\Psi} \left(\frac{R_1 R_2}{s_{12}^2}\right)^{x_\Psi} \quad (2.15a)$$

between distant spheres ($s_{12} \gg R_1, R_2$) and

$$\delta F_{\text{SPW}}(D, R_1) \rightarrow -k_B T_c \frac{A_a^\Psi A_b^\Psi}{B_\Psi} \left(\frac{R_1}{2D}\right)^{x_\Psi} \quad (2.15b)$$

between a planar wall and a single distant sphere ($D \gg R_1$). Here Eqs. (1.4) and (1.9) have been used.

D. Density profiles and short-distance expansion near a planar surface

In this section we study the profile $\langle \Psi(\mathbf{r}') \rangle$ as \mathbf{r}' approaches one of the boundaries of the critical system. The normal component [37] $\langle T_{\perp\perp}(\mathbf{r}') \rangle$ of the stress-tensor average is *regular* near the boundaries [38]. For the concentric geometry, this is apparent from (2.3), and it holds quite generally [39,40]. The behavior of the order parameter and the energy density is quite different, however, and is described by power-law exponents. In general these are determined by the scaling dimensions of surface operators and are different from bulk exponents [25,26]. Here we consider the particularly simple cases where Ψ approaches a *planar* boundary with universality class b and (Ψ, b) is either (Φ, \uparrow) , (Φ^2, \uparrow) , or (Φ^2, O) . Then the leading surface operator is $T_{\perp\perp}$ [8,9,13,30,31], which leads to a surface exponent d

[27,28]. The corresponding short-distance expansion about the planar surface [26] has the form [30,31,39,13]

$$\Psi(\mathbf{r}'_{\parallel}, r'_{\perp}) = A_b^{\Psi} (2r'_{\perp})^{-x_{\Psi}} \left[1 - C_{\Psi}^{(b)} r'_{\perp}^d \lim_{r'_{\perp} \rightarrow 0} T_{\perp\perp}(\mathbf{r}'_{\parallel}, r'_{\perp}) + \dots \right]. \quad (2.16)$$

The planar surface is located in \mathbf{r}' -space at $r'_{\perp} = 0$. The factor in front of the square bracket is the critical half-space profile as in (2.11) for surface universality class b . $C_{\Psi}^{(b)}$ is a universal short-distance amplitude which generally depends on b [41]. Its behavior is known in the Gaussian model with $d > 2$ and in the Φ^4 -theory near the upper critical dimension $d = 4$ [31,13]. The ellipses inside the square brackets in (2.16) denote contributions of higher order in r'_{\perp} . The expansion (2.16) holds in thermal averages or correlation functions where besides the boundary at $r'_{\perp} = 0$ and Ψ other boundaries and operators may be involved.

We are particularly interested in the small r'_{\perp} behavior of $\langle \Psi(\mathbf{r}'_{\parallel}, r'_{\perp}) \rangle_{\text{SPW}}$ in the sphere-near-planar-wall (SPW) geometry, which has been introduced as case (ii) just below Eq. (1.2) and in Eq. (1.9). For the stress tensor

$$\langle T_{\perp\perp}(\mathbf{r}'_{\parallel}, 0) \rangle_{\text{SPW}} = \frac{[D(D + 2R_1)]^{d/2}}{[\mathbf{r}'_{\parallel}^2 + D(D + 2R_1)]^d} Y(\rho), \quad (2.17a)$$

with

$$\rho = \left[D + R_1 - \sqrt{D(D + 2R_1)} \right] / R_1 \quad (2.17b)$$

and D as defined in (1.9). Here we have used the general transformation formula [18,39]

$$\langle T_{\perp\perp}(\mathbf{r}') \rangle = [b(\mathbf{r}')]^{-d} \langle T_{nn}(r) \rangle_{\text{CON}} \quad (2.18a)$$

with the local scale factor

$$b(\mathbf{r}') \equiv \left| \frac{\partial \mathbf{r}}{\partial \mathbf{r}'} \right|^{-1/d} = 1 + \frac{\mathbf{R} \cdot \mathbf{r}'}{R^2} + \frac{r'^2}{4R^2}. \quad (2.18b)$$

Setting $R = R_+$ leads to the SPW geometry on the left hand side of (2.18a) with

$$D(D + 2R_1) = r'_{\perp\text{III}} r'_{\perp\text{IV}} = (2R_+)^2, \quad (2.19)$$

which follows from (1.2). Using the form (2.3) for $T_{nn}(r)$ on the right hand side of (2.18a) and letting $r \rightarrow R_+$ so that $r'_{\perp} \rightarrow 0$ leads to (2.17a). Eq. (2.17b) follows e.g. from (1.5), since the quantity κ from (1.4) equals $1 + D/R_1$ in the SPW case.

We close this section by introducing some of the tools needed in Secs. III and IV. Critical systems with surfaces may be described [26] by a configuration probability $\sim \exp(-\mathcal{H})$ for the fluctuating N -component order parameter $\vec{\Phi}$, where \mathcal{H} separates into a bulk part

$$\mathcal{H}_{\text{bulk}} = \int d^d r \mathcal{L}, \quad \mathcal{L} = \frac{1}{2} \nabla \vec{\Phi} \cdot \nabla \vec{\Phi} + \frac{u}{4!} (\vec{\Phi}^2)^2 \quad (2.20)$$

and surface parts $\mathcal{H}_{\text{surf}}$. While the integration in (2.20) is over the interior of the critical system, e.g. over $R_- < r < R_+$ in the concentric geometry, the surface contributions involve integrals (of powers of Φ and derivatives thereof) over the surfaces of the system. Since we shall only consider systems right at the bulk critical point, we have not included a Φ^2 term in (2.20) [42].

We will also need the explicit form of the stress tensor at an arbitrary interior point of the system. It is given by [43,44]

$$T_{kl}(\mathbf{r}) = (\partial_k \vec{\Phi}) (\partial_l \vec{\Phi}) - \delta_{kl} \mathcal{L} - \mathcal{J}_{kl}, \quad (2.21a)$$

with the canonical tensor supplemented by the improvement term

$$\mathcal{J}_{kl}(\mathbf{r}) = \frac{1}{4} \frac{d-2}{d-1} \left(1 + \mathcal{O}(u_R^3) \right) [\partial_k \partial_l - \delta_{kl} \Delta] \vec{\Phi}^2. \quad (2.21b)$$

The quantity denoted by $\mathcal{O}(u_R^3)$ is needed to renormalize the stress tensor [44]. Since it is of third or higher order in the renormalized coupling u_R (compare Eq. (2.25) below), it does not appear in our explicit low-order calculations.

The thermal average of the stress tensor in the concentric geometry takes the rotationally-invariant form

$$\langle T_{kl}(\mathbf{r}) \rangle_{\text{CON}} = r^{-d} \left[\frac{r_k r_l}{r^2} \tau^{(1)} - \frac{\delta_{kl}}{d} \tau^{(2)} \right]. \quad (2.22)$$

Here $\tau^{(1)}, \tau^{(2)}$ are dimensionless quantities which only depend on the position via $r = |\mathbf{r}|$. A fundamental property of the stress tensor is the continuity equation [44]. In the present case

$$\begin{aligned} 0 &= \sum_l \frac{\partial \langle T_{kl}(\mathbf{r}) \rangle_{\text{CON}}}{\partial r_l} \\ &= r_k r^{-d-2} \left[-(\tau^{(1)} - \tau^{(2)}) + r \frac{d}{dr} \left(\tau^{(1)} - \frac{1}{d} \tau^{(2)} \right) \right], \end{aligned} \quad (2.23)$$

which implies the important relation

$$r \frac{d}{dr} r^d \langle T_{nn}(\mathbf{r}) \rangle_{\text{CON}} = r^d \sum_l \langle T_{ll}(\mathbf{r}) \rangle_{\text{CON}} \quad (2.24)$$

between the r -dependence of the radial component and the trace of the stress tensor. Eqs. (2.23) and (2.24) hold for arbitrary u, d, r and for arbitrary (rotationally-invariant) conditions at the surfaces. If the trace vanishes, as happens [44] if $\mathcal{H}_{\text{bulk}}$ is at the critical fixed point of the renormalization group (RG), Eq. (2.24) implies that $r^d \langle T_{nn} \rangle_{\text{CON}}$ is independent of r . This is consistent with Eq. (2.3).

To set up the RG, we use reparametrization by minimal subtraction of poles in ϵ [45,46,44,26]. We note in particular the relation

$$u = 16\pi^2 \mu^\epsilon u_R [1 + \mathcal{O}(u_R)] \quad (2.25)$$

between the Φ^4 coupling constant u and its renormalized counterpart u_R . Here μ is the inverse length scale that determines the renormalization flow, and the $\mathcal{O}(u_R)$ -contributions contain pole terms in ϵ . The stress tensor (2.21) is already renormalized [44], and quantities such as \mathcal{K} in Eq. (A8) or the functions

$$\tau^{(i)} = \mathcal{G}_d^{(i)}(r/R_+, \rho; \mu r, u_R) \quad (2.26)$$

with $i = 1, 2$ from (2.22) are finite for $\epsilon \rightarrow 0$ order by order in u_R . Eq. (2.26) follows from dimensional analysis, assuming that the boundary condition a, b take their fixed-point form and do not introduce any new lengths. If, in addition, the coupling u_R equals its critical fixed-point value

$$u_R^* = \epsilon \frac{N+2}{N+8} + \mathcal{O}(\epsilon^2), \quad (2.27)$$

the renormalization-group equation [44] implies that the $\tau^{(i)}$ are independent of μr . By Eqs. (2.22)–(2.24) and the vanishing trace, the $\tau^{(i)}$ are also independent of r/R_+ and i . Thus, we find that

$$\mathcal{G}_d^{(i)}(r/R_+, \rho; \mu r, u_R^*) = \mathcal{G}_d^*(\rho) \quad (2.28)$$

only depends on ρ, d and the surface universality classes a, b . This provides another derivation of (2.3).

III. SITUATIONS WITH BROKEN SYMMETRY: MEAN FIELD APPROXIMATION

In this section we consider the surface universality classes $(a, b) = (\uparrow, \uparrow), (\uparrow, \downarrow), (\uparrow, O)$ and (\uparrow, SB) , where the order parameter symmetry is *broken* at the bulk critical point. With applications to the liquid-gas or consolute critical points in mind, we only consider a one-component order parameter. In the standard approach, the order parameter

$$\Phi(\mathbf{r}) = \langle \Phi(\mathbf{r}) \rangle + \varphi(\mathbf{r}) \quad (3.1)$$

is decomposed into a non-vanishing average $\langle \Phi \rangle$ and the fluctuation φ around it. Then a fluctuation (or loop) expansion is carried out, which amounts to an expansion in powers of u .

To leading order one may neglect fluctuations altogether and determine $\langle \Phi \rangle \equiv \langle \Phi \rangle^{(0)}$ by minimizing \mathcal{H} and ignore φ . In the concentric geometry $\langle \Phi \rangle$ only depends on the distance r from the center and [21]

$$\ddot{m} + \frac{d-1}{r} \dot{m} = m^3, \quad (3.2)$$

with

$$m = \sqrt{u/6} \langle \Phi \rangle^{(0)} \quad (3.3)$$

which has the dimension of an inverse length. For the trace of the stress tensor one finds

$$\sum_k \langle T_{kk}(\mathbf{r}) \rangle_{\text{CON}}^{(0)} = -\frac{3}{2} \epsilon m^4/u, \quad (3.4)$$

while the radial component is given by

$$r^d \langle T_{nn}(\mathbf{r}) \rangle_{\text{CON}}^{(0)} = \frac{3}{2} I_d/(ur^\epsilon), \quad (3.5)$$

where

$$I_d = (2\dot{m}^2 - m^4) r^4 + 2(d-2)m\dot{m}r^3. \quad (3.6)$$

Here $\dot{m} \equiv dm/dr$, and the superscript zero denotes the $1/u$ contribution to $\langle T \rangle$, which is obtained by neglecting fluctuations. The first and second term on the right hand side of (3.6) come from the canonical tensor and the improvement term, respectively.

The quantities (3.4) and (3.5) determine the $1/u$ contributions to the right and left hand side of Eq. (2.24), respectively, and allow one to explicitly check (2.24) to this order. Note that for $\epsilon \rightarrow 0$ with $u > 0$ fixed the trace vanishes. Thus I_4 is independent of r and represents a first integral of the differential equation (3.2) if $d = 4$.

This integral was encountered in Ref. [21], where it is pointed out that Eq. (3.2) is a special case of the generalized Emden–Fowler (GEF) equation [47]. For $d = 4$, (3.2) belongs to a subclass of the GEF equation, for which the first integrals are known explicitly [48,47].

A first integral for the mean-field equation in the spherically symmetric geometry may also be constructed by means of the stress tensor if $u\Phi^4$ in (2.20) is replaced by an arbitrary monomial interaction $u\Phi^M$. The leading contribution in u of the stress tensor always has a vanishing trace at the upper critical dimension $d = 2M/(M-2)$ (see Ref. [44]). All the corresponding mean-field equations belong to the above-mentioned subclass.

Now we assume that the boundary conditions for m at $r = R_-$ and $r = R_+$ take their fixed-point forms. Then the dimensionless quantity I_d in (3.6) can only depend upon two ratios, say

$$I_d = I_d(r/R_+, \rho) \quad (3.7)$$

of the three lengths r, R_-, R_+ . In particular, for $d = 4$

$$I_4 = I(\rho), \quad (3.8)$$

i.e., I_4 depends only on ρ . Note that the term in $r^d \langle T_{nn} \rangle_{\text{CON}}$ of leading order in u_R , which follows from substituting (3.7) and (2.25) into (3.5), does indeed have the form (2.26).

The scaling function $Y(\rho)$ in (2.3) follows from $\langle T_{nn} \rangle_{\text{CON}}$ for $u = u_R^*$. Substituting (2.25), (2.27) and (3.8) into (3.5) and keeping only the leading ϵ -dependence, one finds

$$Y(\rho) = \frac{1}{\epsilon} \frac{9}{2\pi^2} I(\rho) + \mathcal{O}(\epsilon^0). \quad (3.9)$$

To obtain solutions m in $d = 4$ with the first integral $I_4 \equiv I$, we follow the procedure in Ref. [21]. With the substitution $m = v/r$ Eq. (3.6) becomes

$$d \ln r = \pm \sqrt{2} \, dv / W(v) , \quad (3.10a)$$

with

$$W(v) = \sqrt{I + 2v^2 + v^4} , \quad (3.10b)$$

and solutions can be obtained in terms of elliptic integrals.

Case (i): For $(a, b) = (\uparrow, \uparrow)$ the order parameter profile m tends to $+\infty$ near the two surfaces and has one minimum in between. This implies $I < 0$ and a solution with the parametric form [21]

$$v = \frac{\sqrt{\gamma - 1}}{\cos \varphi} \quad (3.11a)$$

$$\ln \frac{r}{R_M} = \gamma^{-1/2} F \left(\varphi, [(1 + 1/\gamma)/2]^{1/2} \right) , \quad (3.11b)$$

where F is the elliptic integral

$$F(\varphi, k) = \int_0^\varphi d\hat{\varphi} \left(1 - k^2 \sin^2 \hat{\varphi} \right)^{-1/2} , \quad (3.12)$$

and

$$\gamma = \sqrt{1 - I} . \quad (3.13)$$

Here $r = R_M$ is the radius with minimum v , corresponding to $\varphi = 0$. At $\varphi = \pm\pi/2$ where the profile diverges, r takes the value $r = R_\pm$. Eq. (3.11b) implies $R_- R_+ = R_M^2$ and

$$\ln \rho = -f_1(I) \quad (3.14a)$$

with

$$f_1(I) = 2\gamma^{-1/2} K \left([(1 + 1/\gamma)/2]^{1/2} \right) . \quad (3.14b)$$

Here ρ is from (1.6), and K is the complete elliptic integral

$$K(k) = F(\pi/2, k) . \quad (3.15)$$

Eqs. (3.14), (3.13), and (3.9) determine the scaling function $Y(\rho)$ for the stress tensor in (2.3). Note that I varies from 0 to $-\infty$ as ρ varies from 0 to 1.

Case (ii): The solution for $(a, b) = (SB, \uparrow)$ or (\uparrow, SB) is readily obtained from the solution in (i). Identifying R_M in (3.11b) with the radius of the SB boundary, i.e. considering

$$R_M = R_- < r < R_+ \quad (3.16a)$$

or

$$R_- < r < R_M = R_+ \quad (3.16b)$$

leads to the relation

$$\ln \rho = -\frac{1}{2} f_1(I), \quad (3.17)$$

which only differs from (3.14a) by a factor 1/2. The reason for the identifications (3.16) can be understood by conformally transforming the mean-field (MF) solution (3.11) for (\uparrow, \uparrow) in concentric geometry to spheres of equal size (SES) in \mathbf{r}' -space, with the mid-plane $r'_\perp = 0$ corresponding to the sphere with $r = R_M$ (see the remark just below Eq. (1.2)). The transformed MF solution is invariant under $r'_\perp \rightarrow -r'_\perp$, and the normal derivative vanishes at $r'_\perp = 0$. Since the MF equation $\Delta \langle \Phi \rangle^{(0)} = (u/6) (\langle \Phi \rangle^{(0)})^3$ is conformally invariant in $d = 4$, this is the correct MF solution for a half-space $r'_\perp > 0$ in $d = 4$ with a planar *SB* surface at $r'_\perp = 0$ and a spherical hole with \uparrow boundary conditions. Transforming this solution back to the concentric geometry leads to (3.16) and (3.17). Note that for the two geometries (3.16) the radial derivative $d \ln m(r)/dr$ at the *SB* surfaces does not vanish but equals $-1/R_-$ and $-1/R_+$ for (3.16a) and (3.16b), respectively [49]. Thus the MF order-parameter profile increases (decreases) on approaching the convex (concave) *SB* surface from the interior of the critical system, which is reasonable. The MF values ± 1 for the ratio of the logarithmic normal derivative and the inverse radius of curvature in $d = 4$ are consistent with results in Ref. [50].

Case (iii): For $(a, b) = (\downarrow, \uparrow)$, the profile tends to $\pm\infty$ for $r \rightarrow R_\pm$ and has a zero in between. This implies $I > 0$. Though the I -dependence of $m(r, I)$ is perfectly regular at $I = 1$, it is advantageous to choose different parametric representations for the intervals $0 < I < 1$ and $I > 1$, respectively. They are given by

$$v = (1 - \gamma)^{1/2} \tan \varphi, \quad (3.18a)$$

with

$$\ln \frac{r}{R_0} = \left(\frac{2}{1 + \gamma} \right)^{1/2} F \left(\varphi, [2/(1 + 1/\gamma)]^{1/2} \right) \quad (3.18b)$$

for $0 < I < 1$ (with γ from (3.13)) and by

$$v = I^{1/4} \tan \varphi, \quad (3.19a)$$

with

$$\ln \frac{r}{R_0} = 2^{-1/2} I^{-1/4} F \left(2\varphi, [(1 - I^{-1/2})/2]^{1/2} \right) \quad (3.19b)$$

for $I > 1$. The profile diverges at $\varphi = \pm\pi/2$, corresponding to $r = R_\pm$, and has a zero at $\varphi = 0$, corresponding to $r = R_0 = (R_+ R_-)^{1/2}$. Eqs. (3.18b) and (3.19b) determine the relation $\rho = \rho(I)$. A form which holds for both $0 < I < 1$ and $I > 1$ is

$$\ln \rho = -f_3(I), \quad (3.20a)$$

with

$$f_3(I) = 2^{3/2} I^{-1/4} \frac{2}{\delta} K\left(\frac{2}{\delta} - 1\right). \quad (3.20b)$$

Here

$$\delta = 1 + \left[\left(1 + I^{-1/2} \right) / 2 \right]^{1/2}. \quad (3.21)$$

Case (iv): The solution for $(a, b) = (O, \uparrow)$ follows from that in case (iii) by identifying R_0 with the radius R_- of the O boundary, where the order parameter vanishes [26]. This implies

$$\ln \rho = -\frac{1}{2} f_3(I). \quad (3.22)$$

The four functions $\rho = \rho(I)$ in Eqs. (3.14), (3.17), (3.20), and (3.22) determine via (3.9) the scaling function $Y(\rho)$ of the stress tensor and via (1.8), (1.10), and (2.2) the free energy and the Casimir forces for the four pairs (\uparrow, \uparrow) , (SB, \uparrow) , (\downarrow, \uparrow) , (O, \uparrow) of boundary conditions. Integrating according to (2.2) yields the parametric form

$$\mathcal{F}(\kappa(\rho(I))) = \frac{9 S_d}{2^{d+1} \pi^2 \epsilon} \int_0^I d\hat{I} \frac{d \ln \rho(\hat{I})}{d\hat{I}} \hat{I} \quad (3.23)$$

for the scaling function, with $\kappa = \kappa(\rho)$ from (1.5) and $\rho = \rho(I)$ defined as above. On varying ρ or κ , \mathcal{F} , $\langle T_{nn} \rangle_{\text{CON}}$, and I remain negative in the cases (i) and (ii) and positive in the cases (iii) and (iv), implying attractive and repulsive interactions, respectively. The remaining integration in (3.23) has been carried out numerically. Results for the scaling function for the four combinations of boundary conditions are shown in Fig. 2. Since the prefactor in (3.23) behaves like $1/\epsilon$ as $d \rightarrow 4$, we have plotted the finite quantity $\tilde{\mathcal{F}} = \lim_{d \rightarrow 4} (4 - d) \mathcal{F}$.

It is instructive to check that our solutions exhibit the limiting behavior discussed in Subsecs. II B and II C. Consider first the limit $\rho \rightarrow 1$, where $|I| \rightarrow \infty$. In this case

$$(f_1, f_3) \rightarrow \left(2|I|^{-1/4}, 2^{3/2} I^{-1/4} \right) \cdot K(1/\sqrt{2}). \quad (3.24)$$

Substituting the corresponding $I(\rho)$ into (3.9), one finds that $Y(\rho)$ does indeed have the behavior (2.4b) with $d = 4$ and that

$$\Delta_{\uparrow\uparrow} = -\frac{1}{\epsilon} \frac{3}{2\pi^2} \left[K\left(1/\sqrt{2}\right) \right]^4 \quad (3.25a)$$

and

$$\Delta_{SB\uparrow} = \Delta_{\uparrow\uparrow}/16, \quad \Delta_{\downarrow\uparrow} = -4 \Delta_{\uparrow\uparrow}, \quad \Delta_{O\uparrow} = \Delta_{\downarrow\uparrow}/16. \quad (3.25b)$$

The expressions in (3.25) reproduce the known results [11,13] for the Casimir amplitudes in the parallel-plate geometry for the symmetry-breaking cases and d near 4.

Next consider $\rho \rightarrow 0$, where $|I| \rightarrow 0$. In this case

$$(f_1, f_3) \rightarrow -\ln(|I|/64) \quad (3.26a)$$

which implies

$$I \rightarrow 64 \cdot [-\rho, -\rho^2, \rho, \rho^2] \quad (3.26b)$$

in cases (i)-(iv). In order to compare with (2.13b) we need the expressions

$$\frac{A_a^\Psi A_b^\Psi}{B_\Psi} = \frac{36}{\epsilon} \left[1, \frac{1}{2}, -1, -\frac{1}{2} \right], \quad d \rightarrow 4 \quad (3.27)$$

for AA/B in our four cases. Here $\Psi = [\Phi, \Phi^2, \Phi, \Phi^2]$ as noted just below Eq. (2.13a). The results (3.27) follow from the behavior

$$\pm \sqrt{\frac{12}{uz^2}}, \quad \frac{12}{uz^2}, \quad (3.28)$$

to leading order in u of $\langle \Phi \rangle, \langle \Phi^2 \rangle$ in the half-space with $a = \uparrow$ or \downarrow (see Eq. (2.11)), from the corresponding behavior

$$\mp \tilde{S}_d (2z)^{2-d} \quad (3.29)$$

of $\langle \Phi^2 \rangle$ in the half-space with an $a = O$ or SB surface, and from the leading-order contributions

$$\tilde{S}_d r^{2-d}, \quad 2 \left(\tilde{S}_d r^{2-d} \right)^2 \quad (3.30)$$

to the bulk correlation functions $\langle \Phi \Phi \rangle, \langle \Phi^2 \Phi^2 \rangle$ (cf. Eq. (2.12)). Here

$$\tilde{S}_d = \frac{1}{4} \pi^{-d/2} \Gamma \left(\frac{d}{2} - 1 \right) = \frac{1}{(d-2) S_d}, \quad (3.31)$$

and u must be replaced by (2.25) with the fixed-point value (2.27) with $N = 1$ for u_R . Using the results (3.26b) and (3.27), one finds by means of Eq. (3.9) and from $x_\Phi \rightarrow 1, x_{\Phi^2} \rightarrow 2$ for $d \rightarrow 4$ that our four solutions are indeed consistent with (2.13b).

Now we turn to the density profiles and their behavior near a boundary. Consider first the $r \rightarrow R_+$ behavior of m in the concentric geometry for $d = 4$ with universality class $b = \uparrow$ for the boundary at R_+ . This follows directly from the differential equation (3.10a), which implies

$$\ln \frac{R_+}{r} = \sqrt{2} \int_v^\infty d\hat{v} / W(\hat{v}). \quad (3.32)$$

Here we have used $v(R_+) = \infty$ and assumed that v is larger than a possible minimum in $v(r)$. For r close to R_+ , v tends to infinity, and one may expand the integrand in (3.32) in powers of $1/\hat{v}$. The integration is elementary, and one finds

$$m_{a,\uparrow}(r) = m_\uparrow^{(\text{fc})}(r) \left[1 - \frac{1}{40} I_{a,\uparrow} \left(\frac{R_+ - r}{R_+} \right)^4 + \dots \right]. \quad (3.33)$$

The first factor on the right hand side is the profile inside a full spherical container with radius R_+ , which follows from (3.32) with $I = 0$. The second term in square brackets represents the leading correction for $r \rightarrow R_+$ due to the inner spherical boundary a with

radius R_- . The prefactor $I_{a,\uparrow}$ denotes I in the above cases (i), (ii), (iii), or (iv), with $a = \uparrow$, SB , \downarrow , or O (compare Eq. (3.26b)). The result (3.33) also follows from the parametric representations (3.11b), (3.18b), (3.19b) for $m(r)$.

The corresponding expansion near the planar wall with universality class $b = \uparrow$ in the SPW geometry introduced below (1.2) follows from substituting (3.33) into the transformation formula

$$m_{S_a PW\uparrow}(\mathbf{r}') = [b(\mathbf{r}')]^{-1} m_{a,\uparrow}(r) \quad (3.34)$$

for mean-field solutions in $d = 4$. Here $b(\mathbf{r}')$ is from (2.18b) with $R = R_+$. This leads to the result

$$m_{S_a PW\uparrow}(\mathbf{r}')/m_{PW\uparrow}(r'_\perp) = 1 - \frac{1}{40} I_{a,\uparrow} z^4 + \dots , \quad (3.35)$$

with

$$z = 4 r'_\perp R_+ / \left[(\mathbf{r}'_\parallel)^2 + (2R_+)^2 \right] , \quad (3.36)$$

for the leading behavior of $[R_+ - r(\mathbf{r}')]/R_+$ as $r'_\perp \rightarrow 0$. Here we use the relation between the profiles $m_{PW\uparrow}$ in half-space and $m_{\uparrow}^{(fc)}$ inside a full spherical container that follows from the conformal transformation (3.34) [19]. Using Eqs. (2.17a), (2.17b) and (3.9) for $\langle T_{\perp\perp} \rangle_{SPW}$ and the result [13]

$$C_{\Phi}^{(\uparrow)} = \epsilon \frac{4\pi^2}{45} + \mathcal{O}(\epsilon^2) \quad (3.37)$$

for the universal short-distance amplitude, we have checked that Eqs. (3.35), (3.36) are fully consistent with the short-distance expansion (2.16) when applied to a $\langle \Psi \rangle_{SPW} = \langle \Phi \rangle_{SPW}$ average for $d \rightarrow 4$.

In the other cases such as $(\Psi, b) = (\Phi^2, O)$ with $a = \uparrow$, the short distance expansion (2.16) about the planar wall with universality class b can be checked in a similar way [51]. The short-distance coefficient $C_{\Phi^2}^{(O)}$ turns out [31] to be of order ϵ^0 (see Eq. (4.24) below). As a consequence, the first term in square brackets in (2.16) leads to a contribution which is smaller by a factor ϵ than the contribution from the second term and is not present in the mean-field solution.

In Appendix B 1 we evaluate density profiles for $R_- \rightarrow 0$ for arbitrary fixed $0 < r < R_+$.

For $\rho \rightarrow 1$, the density profile in the parallel-plate geometry [11] is obtained. This has been shown for $(a, b) = (\uparrow, \uparrow)$ in Ref. [21], and similar arguments apply for other a, b .

IV. SITUATIONS WITH SYMMETRY PRESERVED: GAUSSIAN MODEL

The boundary conditions $(a, b) = (O, O)$, (O, SB) , (SB, SB) do not destroy [26] the bulk $O(N)$ symmetry of the N -component order parameter at the bulk critical point. In these cases the starting point of the $d = 4 - \epsilon$ expansion is [45] the critical Gaussian model. This is defined by Eq. (2.20) with $u = 0$. It is instructive [52] to consider the critical Gaussian model for arbitrary $d > 2$. For all d it is at its critical fixed point, i.e. dilatation

and conformally invariant on all length scales. This also holds in the presence of boundaries a and b if the boundary conditions take their fixed-point forms.

In the concentric geometry the Gaussian order-parameter correlation functions or ‘propagators’ with $a, b \in \{O, SB\}$,

$$\langle \Phi_i(\mathbf{r}_1) \Phi_j(\mathbf{r}_2) \rangle_{\text{CON}} = \delta_{ij} G_{ab}(\mathbf{r}_1, \mathbf{r}_2) = \delta_{ij} \tilde{G}_{ab}(r_1, r_2; \eta) , \quad (4.1)$$

only depend on the positions $\mathbf{r}_1, \mathbf{r}_2$ through their distances r_1, r_2 from the center and the cosine of the enclosed angle

$$\eta = \mathbf{r}_1 \cdot \mathbf{r}_2 / (r_1 r_2) . \quad (4.1a)$$

Here i and j denote components of the order parameter. One finds

$$\tilde{G}_{ab}(r_1, r_2; \eta) = \tilde{S}_d (r_< r_>)^{-\vartheta} \sum_{l=0}^{\infty} C_l^{(\vartheta)}(\eta) W_{a,b}^{(l)} \chi_a((r_</R_-)^\lambda) \chi_b((r_>/R_+)^\lambda) \quad (4.2)$$

with

$$r_< = \min(r_1, r_2) , \quad r_> = \max(r_1, r_2) \quad (4.2a)$$

and

$$\vartheta = (d - 2)/2 . \quad (4.2b)$$

The $C_l^{(\vartheta)}$ are hyperspherical (Gegenbauer) polynomials [53], and

$$\chi_O(y) = y - \frac{1}{y} , \quad \chi_{SB}(y) = y + \frac{1}{y} \quad (4.2c)$$

and

$$\lambda = l + \vartheta . \quad (4.2d)$$

The quantities W depend on the ratio $\rho = R_-/R_+$ of the radii of concentric boundaries and are given by

$$\begin{aligned} W_{O,O}^{(l)} &= - [P^{-1} - P]^{-1} \\ W_{O,SB}^{(l)} &= [P^{-1} + P]^{-1} \\ W_{SB,O}^{(l)} &= - [P^{-1} + P]^{-1} \\ W_{SB,SB}^{(l)} &= [P^{-1} - P]^{-1} , \end{aligned} \quad (4.2e)$$

with

$$P = \rho^\lambda . \quad (4.2f)$$

The $G_{ab}(\mathbf{r}_1, \mathbf{r}_2)$ remain unchanged for $\mathbf{r}_1 \leftrightarrow \mathbf{r}_2$ and satisfy $\Delta_{\mathbf{r}_1} G_{ab} = -\delta(\mathbf{r}_1 - \mathbf{r}_2)$ with Δ and δ the Laplacian and the Dirac δ -function, respectively, in d dimensions. Note that χ_O and $\partial\chi_{SB}/\partial y$ vanish at the boundaries where $y = 1$. This implies the fixed-point boundary conditions

$$G_{O,b} = 0, \quad G_{a,O} = 0 \quad (4.3)$$

and [50]

$$\partial_{r_<} G_{SB,b} = -\frac{\vartheta}{R_-} G_{SB,b}, \quad \partial_{r_>} G_{a,SB} = -\frac{\vartheta}{R_+} G_{a,SB}. \quad (4.4)$$

Here the first and second relations in (4.3) and (4.4) hold for $r_< = R_-$ and $r_> = R_+$, respectively.

A conformal transformation

$$G_{ab}^{(\text{SPW})}(\mathbf{r}'_1, \mathbf{r}'_2) = [b(\mathbf{r}'_1) b(\mathbf{r}'_2)]^{-\vartheta} G_{ab}(\mathbf{r}_1, \mathbf{r}_2) \quad (4.5)$$

to the sphere near the planar wall (SPW) geometry shows that (4.4) is equivalent to the usual Neumann boundary condition for a planar SB surface: Consider e.g. (1.1) with $R = R_+$, which transforms the outer concentric boundary $b = SB$ to the plane $r'_\perp = 0$ (see Fig. 1). To prove that the derivative vanishes at $r'_{1\perp} = 0$ for $r'_{2\perp} > 0$, we show that the continuation in $r'_{1\perp}$ of $G^{(\text{SPW})}$ across the boundary is even in $r'_{1\perp}$. The points corresponding to $\mathbf{r}'_1 = (\mathbf{r}'_{1\parallel}, r'_{1\perp})$ and its mirror image $\mathbf{r}'^{(I)}_1 = (\mathbf{r}'_{1\parallel}, -r'_{1\perp})$ are \mathbf{r}_1 and

$$\mathbf{r}'^{(I)}_1 = \mathbf{r}_1 R_+^2/r_1^2, \quad (4.6)$$

respectively, as follows from inversion about the sphere $r = R_+$. Since

$$\chi_{SB}\left((r'_1/R_+)^{\lambda}\right) = \chi_{SB}\left((r_1/R_+)^{\lambda}\right) \quad (4.7)$$

and

$$r'_1 b(\mathbf{r}'^{(I)}_1) = r_1 b(\mathbf{r}'_1), \quad (4.8)$$

Eq. (4.5) shows that $G^{(\text{SPW})}$ is indeed even in $r'_{1\perp}$.

An inversion about the sphere $r = \sqrt{R_- R_+}$ exchanges the boundaries a and b and implies

$$\tilde{G}_{ba}(r_1, r_2; \eta) = \left(\frac{R_- R_+}{r_1 r_2}\right)^{2\vartheta} \tilde{G}_{ab}\left(\frac{R_- R_+}{r_1}, \frac{R_- R_+}{r_2}; \eta\right). \quad (4.9)$$

One easily verifies that $\tilde{G}_{O,SB}$, $\tilde{G}_{SB,O}$ in (4.2) are consistent with (4.9).

G_{ab} in (4.2) should be compared with the propagator in the unbounded bulk

$$G_{\text{bulk}}(\mathbf{r}_1, \mathbf{r}_2) = \tilde{S}_d |\mathbf{r}_1 - \mathbf{r}_2|^{-2\vartheta} = \tilde{S}_d (r_< r_>)^{-\vartheta} \sum_{l=0}^{\infty} C_l^{(\vartheta)}(\eta) (r_</r_>)^{\lambda}. \quad (4.10)$$

This equation follows from G_{ab} in (4.2) in the limits $R_- \rightarrow 0$, $R_+ \rightarrow \infty$ with $\mathbf{r}_1, \mathbf{r}_2$ fixed. Below we will need the difference

$$G_{ab}(\mathbf{r}_1, \mathbf{r}_2) - G_{\text{bulk}}(\mathbf{r}_1, \mathbf{r}_2) = \tilde{S}_d \sum_{l=0}^{\infty} C_l^{(\vartheta)}(\eta) \left[\sigma_{ab}^{(1)} P^{-2} - 1 \right]^{-1} \cdot \left\{ \frac{r_1^l}{r_2^{\vartheta+\lambda}} + \frac{r_2^l}{r_1^{\vartheta+\lambda}} + \sigma_{ab}^{(2)} \frac{(r_1 r_2)^l}{R_-^{2\lambda}} + \sigma_{ab}^{(3)} \frac{R_+^{2\lambda}}{(r_1 r_2)^{\vartheta+\lambda}} \right\}, \quad (4.11)$$

which is regular for $\mathbf{r}_1 \rightarrow \mathbf{r}_2$ at interior points. Here

$$\begin{aligned} \sigma_{ab}^{(1)} &= (1, -1, -1, 1) \\ \sigma_{ab}^{(2)} &= (-1, -1, 1, 1) \\ \sigma_{ab}^{(3)} &= (-1, 1, -1, 1) \end{aligned} \quad (4.11a)$$

for

$$ab = (O \ O, O \ SB, SB \ O, SB \ SB). \quad (4.11b)$$

In order to calculate $\langle T_{nn}(r) \rangle_{\text{CON}}$ in the Gaussian model, we use (2.21a) with $u = 0$ in the Hamiltonian (2.20). Since the average $\langle T_{kl} \rangle_{\text{bulk}}$ in the unbounded bulk vanishes, we evaluate the averages $\langle \Phi \Phi \rangle_{\text{CON}}$ and $\langle \Phi^2 \rangle_{\text{CON}}$ that arise from Eq. (2.21a) by using $G_{ab} - G_{\text{bulk}}$ from (4.11) instead of G_{ab} . This yields

$$\begin{aligned} N^{-1} \langle T_{nn}(\mathbf{r}) \rangle_{\text{CON}} &= \\ -r^{-d} \tilde{S}_d \sum_{l=0}^{\infty} \left[\sigma_{ab}^{(1)} P^{-2} - 1 \right]^{-1} \binom{d-3+l}{l} &\left\{ 2l(d-2+l) + \frac{1}{2}(d-2)^2 \right\}. \end{aligned} \quad (4.12)$$

Using (2.2), one eventually obtains

$$N^{-1} \mathcal{F}(\kappa) = \frac{1}{d-2} \sum_{l=0}^{\infty} \ln \left(1 - \sigma_{ab}^{(1)} \rho(\kappa)^{2\lambda} \right) \frac{1}{2\lambda} \binom{d-3+l}{l} \left\{ 2l(d-2+l) + \frac{1}{2}(d-2)^2 \right\} \quad (4.13)$$

where the relation between κ and ρ is given in (1.5). The signs of both \mathcal{F} and $\langle T_{nn} \rangle_{\text{CON}}$ are opposite to the sign of $\sigma_{ab}^{(1)}$. This holds for all values of κ or ρ . Thus the interaction is always attractive if $a = b$ and repulsive if $a \neq b$. We have evaluated numerically the sum in (4.13). The function $-\mathcal{F}_{O,O} = -\mathcal{F}_{SB,SB}$ for $d = 4$ is shown in Fig. 2.

The profile of the energy density [36] is obtained from $G_{ab} - G_{\text{bulk}}$. It takes the form

$$\begin{aligned} N^{-1} \langle \vec{\Phi}^2(\mathbf{r}) \rangle_{\text{CON}} &= \\ r^{2-d} \tilde{S}_d \sum_{l=0}^{\infty} \left[\sigma_{ab}^{(1)} P^{-2} - 1 \right]^{-1} \binom{d-3+l}{l} &\left\{ 2 + \sigma_{ab}^{(2)} \left(\frac{r}{R_-} \right)^{2\lambda} + \sigma_{ab}^{(3)} \left(\frac{R_+}{r} \right)^{2\lambda} \right\}. \end{aligned} \quad (4.14)$$

Note the different sources of r -dependence in the expression (4.14) for the energy density. The r -dependence is very similar in each of the contributions to $\langle T_{nn} \rangle$ coming from Eqs. (2.21). However, $(r/R_-)^{2\lambda}$ and $(R_+/r)^{2\lambda}$ cancel in the sum, and $\langle T_{nn} \rangle$ in (4.12) turns out proportional to r^{-d} , in agreement with (2.3). The $(\partial\Phi)^2$ terms with ∂ parallel or perpendicular to \mathbf{r} that arise from the canonical tensor in (2.21a) contribute half of the first

term in the curly brackets on the right hand side of (4.12), while the second term comes from the improvement \mathcal{J} in (2.21b). The sum of the two terms in curly brackets equals $2\lambda^2$.

From (4.12) and (4.14), one may again check that the two combinations $(a, b) = (O, SB)$ and (SB, O) are related by an inversion about the sphere $r = \sqrt{R_- R_+}$. This operation preserves $\langle T_{nn} \rangle$, while in $\langle \Phi^2 \rangle$ the ratios r/R_- and R_+/r are exchanged. Note that $\langle T_{nn} \rangle$ is the same for (O, O) and (SB, SB) , too. However, the latter identity is limited to the Gaussian model, as we argue below.

We now consider the limiting behavior of the stress tensor in (4.12). According to the discussion in Subsec. II B, $\langle T_{nn} \rangle$ should approach the parallel-plate result when $\rho = 1 - (L/R_+)$ tends to 1. In this case

$$P^{-2} \approx \exp(2\lambda L/R_+) . \quad (4.15)$$

The exponential decay of the first factor in (4.12) is very slow, and the sum in (4.12) may be replaced by an integral

$$\sum_l \longrightarrow \int_0^\infty dl \left[\sigma_{ab}^{(1)} P^{-2} - 1 \right]^{-1} 2 l^{d-1} / \Gamma(d-2) . \quad (4.16)$$

Here P^{-2} is from (4.15) with λ replaced by l , and the second and third factors in the sum of (4.12) have been replaced by their limiting forms for $l \gg 1$. The integral in (4.16) can be expressed in terms of the Riemann zeta function $\zeta(d)$ [54]. Comparison with Eqs. (2.3) and (2.4b) shows that $\langle T_{nn} \rangle$ does indeed have the expected limiting form, with the well-known Casimir amplitudes [10,12]

$$\Delta_{O,O} = \Delta_{SB,SB} = -N (4\pi)^{-d/2} \Gamma\left(\frac{d}{2}\right) \zeta(d) \quad (4.17a)$$

and

$$\Delta_{O,SB} = -\left(1 - 2^{1-d}\right) \Delta_{O,O} \quad (4.17b)$$

for the N -component Gaussian model bounded by plates of type O or SB .

In the other limit $\rho \rightarrow 0$ the leading behavior of (4.12) comes from the $l = 0$ term in the sum, which is given by

$$\sum_l \longrightarrow \sigma_{ab}^{(1)} \rho^{2\vartheta} \frac{1}{2} (d-2)^2 . \quad (4.18)$$

This should be compared with the amplitude ratios

$$A_a^{\Phi^2} A_b^{\Phi^2} / B_{\Phi^2} = \sigma_{ab}^{(1)} N/2 \quad (4.19)$$

for the combinations (4.11b) of a and b . These follow from Eqs. (3.29) and (3.30). Comparing with (2.3) and (3.31), one obtains the expected limiting behavior (2.13b) with $x_{\Phi^2} = d - 2$.

We conclude the discussion of $\langle T_{nn} \rangle_{\text{CON}}$ in the limits $\rho \rightarrow 1$ and $\rho \rightarrow 0$ with two remarks: (i) Only the canonical part of T_{kl} , i.e. the first term in curly brackets in (4.12), contributes in the limit $\rho \rightarrow 1$. This is to be expected, since the average of the improvement term, which

contains a total derivative parallel to the plates, vanishes due to translational invariance in the parallel-plate geometry. It is less obvious that the leading behavior for $\rho \rightarrow 0$ is only due to the improvement term (second term in curly brackets in (4.12)), as we have noted in Eq. (4.18). (ii) For a normal critical system the Φ^4 -interaction of (2.20) must be included. Then $\langle T_{nn} \rangle$ and thus Y and \mathcal{F} for (O, O) and (SB, SB) are no longer the same. From (2.13b) there should already be a deviation in first order in $\epsilon = 4 - d$ for $\rho \rightarrow 0$, since

$$\left(A_{SB}^{\Phi^2} / A_O^{\Phi^2} \right)^2 = 1 + 2\epsilon \frac{N+2}{N+8} + \mathcal{O}(\epsilon^2). \quad (4.20)$$

However, for $\rho \rightarrow 1$, i.e. in the parallel-plate geometry there is no deviation in this order [12].

Now we turn to the profile (4.14) of the energy density. This is the counterpart of the discussion at the end of Sec. III. For r fixed and $R_- \rightarrow 0$ only the second term in curly brackets in Eq. (4.14) survives, and the concentric profile tends to

$$\begin{aligned} N^{-1} \langle \vec{\Phi}^2(\mathbf{r}) \rangle_{\text{CON}} &\longrightarrow r^{2-d} \sigma_{ab}^{(3)} \tilde{S}_d \sigma_{ab}^{(3)} \sum_{l=0}^{\infty} \binom{d-3+l}{l} \left(\frac{r}{R_+} \right)^{2l} \\ &= \sigma_{ab}^{(3)} \tilde{S}_d \left\{ R_+ \left[1 - \left(\frac{r}{R_+} \right)^2 \right] \right\}^{-(d-2)} = N^{-1} \langle \vec{\Phi}^2(\mathbf{r}) \rangle_{\text{fc}}, \end{aligned} \quad (4.21)$$

which is the profile inside a full spherical container (fc) with radius R_+ and universality class b (see the corresponding general expression in Ref. [19]). Below we will need the difference

$$\begin{aligned} N^{-1} \left[\langle \vec{\Phi}^2(\mathbf{r}) \rangle_{\text{CON}} - \langle \vec{\Phi}^2(\mathbf{r}) \rangle_{\text{fc}} \right] &= \\ r^{2-d} \tilde{S}_d \sum_{l=0}^{\infty} \left[\sigma_{ab}^{(1)} P^{-2} - 1 \right]^{-1} \binom{d-3+l}{l} \left\{ 2 + \sigma_{ab}^{(3)} \left[\left(\frac{r}{R_+} \right)^{2\lambda} + \left(\frac{R_+}{r} \right)^{2\lambda} \right] \right\} &. \end{aligned} \quad (4.22)$$

Note that the second term in curly brackets is different from that in (4.14).

Here we study the behavior for $r \rightarrow R_+$ with $b = O$, $\sigma_{ab}^{(3)} = -1$. In this case the expression in curly brackets in (4.22) tends to $-4\lambda^2 [(R_+ - r)/R_+]^2$, and the sum over l can be expressed in terms of $\langle T_{nn} \rangle$ in (4.12). Using (2.3), this leads to

$$\langle \vec{\Phi}^2(r) \rangle_{\text{CON}} \longrightarrow \langle \vec{\Phi}^2(r) \rangle_{\text{fc}} \left[1 - \frac{1}{2} \tilde{S}_d^{-1} N^{-1} Y(\rho) \left(\frac{R_+ - r}{R_+} \right)^d + \dots \right] \quad (4.23)$$

for $r \rightarrow R_+$ and $b = O$. This is the counterpart of (3.33). As in Eqs. (3.34)–(3.37), one may transform to an SPW geometry and identify the leading coefficient $C_{\Phi^2}^{(O)}$ in the short-distance expansion (SDE) about the planar wall with $b = O$. Now exponents $-(d-2)$ and d instead of -1 and 4 appear in Eqs. (3.34) and (3.35), respectively, and

$$C_{\Phi^2}^{(O)} = 2^{d-1} / (N \tilde{S}_d). \quad (4.24)$$

This result, obtained here from the $S_a \text{PW}_O$ geometry with $a = O$ or SB , is consistent with the result for $S_\uparrow \text{PW}_O$ geometry for $d \rightarrow 4$, discussed in the paragraph after Eq. (3.37). It

is also in agreement with Refs. [3,31], where the SDE of Φ^2 about an O surface has been applied to the profile in the parallel-plate geometry and in the half-space at $T > T_c$ and to correlation functions in the half-space at T_c . In Ref. [31] $C_{\Phi^2}^{(O)}$ for the Gaussian model was called \mathcal{B} .

Eq. (4.22) can also be used to evaluate the density profiles for arbitrary fixed $0 < r < R_+$ as $R_- \rightarrow 0$, and one may check the predictions of the small-sphere expansion. This is done in Appendix B 2.

Finally, we mention that for $\rho \rightarrow 1$ the profiles (4.14) of the energy density reduce to the Gaussian results in the parallel-plate geometry [3,31]. This may be shown with arguments analogous to those near Eqs. (4.15) and (4.16).

V. SUMMARY AND CONCLUDING REMARKS

We have analyzed the Casimir interaction between two spherical particles in a fluid at the critical point with boundary conditions

$$(a, b) = (\uparrow, \uparrow), (\uparrow, \downarrow), (\uparrow, O), (\uparrow, SB), (O, O), (O, SB), (SB, SB).$$

The Casimir interaction is completely determined by a universal function $\mathcal{F} = \mathcal{F}_{a,b}$ of a single variable κ (see Eq. (1.4)), which is a combination of the three lengths that characterize the configuration of two spheres.

We have discussed the limiting behavior for spheres that nearly touch ($\kappa \rightarrow 1$) and spheres that are far apart from each other ($\kappa \rightarrow \infty$) and calculated the complete functions $\mathcal{F}_{ab}(\kappa)$ for the case where the spatial dimension d is near 4 [55] (see Fig. 2). From these results and corresponding information for $d = 2$ and $(a, b) = (\uparrow, \uparrow), (\uparrow, \downarrow), (\uparrow, O), (O, O)$ [14], one can make fairly reliable estimates of the scaling functions \mathcal{F}_{ab} in $d = 3$.

Since κ and \mathcal{F} are unchanged under conformal coordinate transformations, it is sufficient to consider a critical system bounded by two concentric spheres. We have derived $\mathcal{F}(\kappa)$ by calculating the average of the stress-energy tensor in this highly symmetric geometry.

Besides the global free energy local thermodynamic averages, e.g. profiles of the order parameter and the energy density in the presence of two spherical particles, are also of interest. These can also be derived from the concentric geometry [21], and we have presented explicit results for d near 4 and for various surface universality classes a, b . We have also demonstrated that the stress-tensor average determines the modification of the density profile near the surface of one sphere due to the other distant sphere [1,30].

The Casimir interaction and the density profiles for parallel plates are obtained as a special case of the results for concentric spheres when the radii R_-, R_+ tend to infinity with fixed difference $R_+ - R_-$ (compare Fig. 1 a). The other extreme $R_- \rightarrow 0$ with R_+ fixed is also of interest. It determines the Casimir effect and the density profiles when one sphere is much smaller than other lengths in the problem. We have checked that the free energy contribution and the density profiles arising from the presence of the small sphere are consistent with a ‘small-sphere operator expansion’. This method has been introduced in Ref. [14] and is also explained in Sec. II C of this paper. The density profiles show still non-trivial scaling forms in this limit (cf. Appendix B).

We have also found simple expressions [35] for the interaction between distant spheres in an infinite host fluid if the latter is not at the critical point. Here both the host correlation length ξ and the distance s between the spheres have to be much larger than the radii of the spheres, but the ratio ξ/s is unrestricted. Similar expressions have been found for the interaction of a single sphere with a distant planar boundary.

We conclude by discussing possible experimental observations of Casimir interactions between spheres at the critical point. The case of fluid mixtures at their consolute point is of particular interest, since the attractive interaction between two immersed equal spheres decays extremely slowly, with a power law

$$-k_B T_c \mathcal{A} (s_{12}/R_1)^{-1.04} \quad (5.1)$$

in $d = 3$ as the separation s_{12} becomes much larger than the radius R_1 of the spheres. The exponent follows from Eq. (2.15a), with $2x_\Phi \equiv 2\beta/\nu = 1.04$ in $d = 3$ [56]. In the only previous theoretical work we know on this topic, de Gennes [2] obtained an extremely good estimate 1 for this exponent by minimizing a phenomenological free energy functional. The universal amplitude $\mathcal{A} = (A_\uparrow^\Phi)^2 / B_\Phi$ is estimated to be somewhat larger than $\sqrt{2}$ [14]. The Casimir interaction (5.1) should be compared with the van der Waals interaction which decays much faster with an exponent -6 (non-retarded) or -7 (retarded). The prefactors are comparable. For example, for fused silica spheres in water the van der Waals prefactor is about $-k_B \cdot 10^3$ Kelvin [57]. We note that for spheres in ${}^4\text{He}$ at the λ -point (XY model) the Casimir exponent is $2x_{\Phi^2} \equiv 2(d - 1/\nu) = 3.02$ for $d = 3$. Thus the decay is faster than for fluid mixtures (see (5.1)).

Finally we mention two classes of experiments one could conceivably carry out to study the Casimir interaction:

- (i) Interaction between only two objects, for example a single sphere near a planar wall: By measuring the force on the sphere for varying distance from the wall, one can in principle obtain the whole scaling function $\mathcal{F}(\kappa)$. Of course, the distance must not exceed the correlation length of the nearly critical host binary fluid. Correlation lengths of several 1000 Å are feasible, and one would like to have a sphere diameter of a few hundred Å. Measurements of the interaction potential of isolated pairs of spheres of somewhat larger size have been reported for a charge stabilized colloid [58], see also [16].
- (ii) Aggregation phenomena in colloids: The Casimir interaction between more than two spherical particles at large [59] separations is a sum of pair interactions, which have the gravitation-like form (5.1) for separations s smaller than the correlation length ξ of the pure host and vanish for $s \gg \xi$. On approaching the critical point ξ strongly exceeds the radii and mean separation of colloid particles. This offers a possible mechanism for their aggregation [60].

Acknowledgements: We thank W. Fenzl, M. Lässig, H. Wagner, and especially T. W. Burkhardt for helpful comments and discussions. We also thank T. W. Burkhardt for a critical reading of the manuscript. U. R. would like to thank the Deutsche Forschungsgemeinschaft for partial support through Sonderforschungsbereich 237.

Note added in proof: After this work was completed we realized that the widely

used non-retarded Hamaker approximation δE for the van der Waals interaction of two spheres is also *conformally invariant* (like the critical Casimir energy δF studied in this paper). This follows immediately from its representation $-(A/\pi^2) \int d^3r_1 d^3r_2 |\mathbf{r}_1 - \mathbf{r}_2|^{-6}$ with integrations over the two spheres and allows to express δE as a function of the invariant quantity κ defined in (1.4). The explicit result [57] $\delta E(s_{12}, R_1, R_2) = -(A/6) \{(\kappa-1)^{-1} + (\kappa+1)^{-1} + \ln[(\kappa-1)/(\kappa+1)]\}$ may be used for a first comparison of critical Casimir and van der Waals interaction. Note that for *close* spheres (κ near 1) δE has the *same* dependence on R_1, R_2, D as δF and can be obtained from the right hand side of (2.5) by replacing $k_B T_c S_d \Delta_{ab}$ by $-A/3$ and setting $d = 3$.

APPENDIX A: FREE ENERGY AND STRESS-TENSOR AVERAGE

An infinitesimal coordinate transformation

$$\hat{\mathbf{x}} = \mathbf{x} + \mathbf{a}(\mathbf{x}) \quad (\text{A1})$$

changes a geometry G to a geometry \hat{G} . We consider two examples:

(i) For the geometry of non-overlapping spheres in Fig. 1 b where $\mathbf{x} = \mathbf{r}'$,

$$a_i(\mathbf{r}) = \alpha \delta_{i,\perp} \Theta(r'_\perp) , \quad (\text{A2})$$

with Θ the unit step function, implies a rigid shift of the right sphere in the \perp direction and increases the distance s_{12} between the spheres by the amount α .

(ii) For the concentric geometry in Fig. 1 a where $\mathbf{x} = \mathbf{r}$, we consider the transformation (2.1).

The corresponding change in the singular part of the free energy is given by [18]

$$F_{\hat{G}} = F_G - k_B T_c \int d^d x \sum_{kl} (\partial a_k(\mathbf{x}) / \partial x_l) \langle T_{kl}(\mathbf{x}) \rangle_G \quad (\text{A3})$$

to first order in α . Here T_{kl} is the stress tensor. In case (i)

$$-\frac{\partial}{\partial s_{12}} \delta F(s_{12}, R_1, R_2) / k_B T_c = \int d^{d-1} r'_\parallel \langle T_{\perp\perp}(r'_\parallel, 0) \rangle , \quad (\text{A4})$$

with the average taken in the geometry of Fig. 1 b. In case (ii)

$$\partial a_k / \partial r_l = \alpha \left[\delta_{kl} \Theta(r - r_0) + \frac{r_k r_l}{r} \delta(r - r_0) \right] . \quad (\text{A5})$$

The result simplifies at the critical fixed point since the trace of the stress tensor vanishes for $R_- < r < R_+$ [18]; a possible boundary contribution at $r = R_+$ drops out in the change of δF_{CON} [23]. Then only the second term on the right hand side of (A5) contributes and picks out the radial component T_{nn} of the stress tensor. This leads to

$$\frac{d}{d\alpha} F_{\text{CON}} (R_- / [(1 + \alpha) R_+]) \Big|_{\alpha=0} = -k_B T_c S_d r_0^d \langle T_{nn}(r_0) \rangle_{\text{CON}} \quad (\text{A6})$$

to first order in α , which implies Eq. (2.2).

Since both $\delta F(s_{12}, R_1, R_2)$ and $\delta F_{CON}(\rho)$ can be expressed in terms of the same function $\mathcal{F}(\kappa)$ (see Sec. I), the ratio between the left-hand sides of Eqs. (A4) and (2.2) is simply $-(\partial\kappa/\partial s_{12})/(\rho d\kappa(\rho)/d\rho)$, with κ and $\kappa(\rho)$ from (1.4) and (1.5), respectively. It is instructive to verify from the transformation formula (2.18a) for the stress-tensor average at the critical fixed point that the right-hand sides of (A4) and (2.2) lead to the same simple ratio. With $r'_\perp = \mathbf{R} \cdot \mathbf{r}' = 0$ and $r = R$ in Eq. (2.18a), an easy r'_\parallel -integration leads to the ratio $1/(2R)$. This equals the above-mentioned ratio, since

$$2R \frac{s_{12}}{R_1 R_2} = \frac{1}{2} (\rho^{-1} - \rho) \quad (\text{A7})$$

as follows from writing s_{12} , R_1 , R_2 in terms of the intersection points I, II, III, IV in (1.2).

Eq. (A4) is not restricted to the critical fixed point but applies for arbitrary values u_R of the renormalized Φ^4 coupling strength (see Eq. (2.25)). This can be used to show the universality (u_R -independence) of the singular part of the free energy in the long-distance limit. For simplicity consider a situation where the boundary conditions have their fixed-point form. Then by naive dimensional analysis the right hand side of (A4) can be written as

$$\int d^{d-1}r'_\parallel \langle T_{\perp\perp}(r'_\parallel, 0) \rangle = \frac{1}{s_{12}} \mathcal{K}(R_1/s_{12}, R_2/s_{12}; \mu s_{12}, u_R). \quad (\text{A8})$$

In the ‘shift operator’ $\int d^{d-1}r'_\parallel T_{\perp\perp}(r'_\parallel, 0)$ the improvement term \mathcal{J} in (2.21b) does not contribute, and the average (A8) is renormalized and obeys a simple *homogeneous* renormalization group equation [44]

$$\left[\mu \frac{\partial}{\partial \mu} + \beta(u_R) \frac{\partial}{\partial u_R} \right] \mathcal{K}(R_1/s_{12}, R_2/s_{12}; \mu s_{12}, u_R) = 0 \quad (\text{A9})$$

with the usual β -function [45,46]. Standard arguments then imply that in the long-distance (infrared) limit $\mu s_{12} \rightarrow \infty$ with R_1/s_{12} and R_2/s_{12} fixed

$$\mathcal{K}(R_1/s_{12}, R_2/s_{12}; \mu s_{12}, u_R) \longrightarrow \mathcal{K}(R_1/s_{12}, R_2/s_{12}; 1, u_R^*) \quad (\text{A10})$$

with u_R^* from (2.27). This shows the u_R -independence of the asymptotic critical Casimir force (A4).

APPENDIX B: DENSITY PROFILES AND SMALL-SPHERE EXPANSION

Here we study the density profiles $\langle \tilde{\Psi} \rangle_{CON} \equiv \langle \tilde{\Psi} \rangle_{a,b}$ in the concentric geometry in the limit $R_- \rightarrow 0$ with $\tilde{r} = r/R_+$ fixed at an arbitrary positive value $0 < \tilde{r} < 1$. We show that this form is indeed in agreement with [33], i.e.

$$\langle \tilde{\Psi}(\mathbf{r}) \rangle_{a,b} - \langle \tilde{\Psi}(\mathbf{r}) \rangle_{fc} \longrightarrow \frac{A_a^\Psi}{B_\Psi} (R_-)^{x_\Psi} \left[\langle \Psi(0) \tilde{\Psi}(\mathbf{r}) \rangle_{fc} - \langle \Psi(0) \rangle_{fc} \langle \tilde{\Psi}(\mathbf{r}) \rangle_{fc} \right], \quad (\text{B1})$$

which follows from the small-sphere expansion (SSE) (2.9), (2.6b), and (2.10). As before the full container (fc) has a surface with universality class b . In (B1), $\Psi = \Phi$ if both A_a^Φ and the correlation in square brackets are non-vanishing, and $\Psi = \Phi^2$ otherwise.

1. Cases with broken symmetry for $d \rightarrow 4$

We start with the two cases $(a, b) = (\uparrow, O)$ and (\uparrow, SB) , where only the inner sphere breaks the symmetry. Consider first $\tilde{\Psi} = \Phi$. Then $\Psi = \Phi$, and (B1) implies

$$\langle \Phi(\mathbf{r}) \rangle_{\uparrow, b}^{(0)} = \sqrt{\frac{6}{u}} \frac{v(r)}{r} \quad (\text{B2a})$$

with

$$v(r) \longrightarrow 2\sqrt{2} \rho q_{\mp} \quad \text{where} \quad q_{\mp} = \tilde{r}^{-1} \mp \tilde{r}. \quad (\text{B2b})$$

Here the upper sign holds for $b = O$ and the lower sign for $b = SB$. To obtain (B2) we have used the vanishing of $\langle \Phi \rangle_{\text{fc}}$ for $b = O$ and SB and the result for $\langle \Phi(0)\Phi \rangle_{\text{fc}}$ that follows via a simple conformal transformation [19] from the half-space correlation function, which for $d \rightarrow 4$ is that of the Gaussian model with Dirichlet or Neumann boundary conditions [26]. We have also used (3.28) and (3.30) to evaluate A_{\uparrow}^{Φ} and B_{Φ} , respectively.

The predictions (B2) of the SSE are consistent with the solutions of the differential equation (3.10a). For $b = O$ this has the form

$$\ln \frac{R_+}{r} = \sqrt{2} \int_0^v \frac{d\hat{v}}{W(\hat{v})}. \quad (\text{B3})$$

Note that I is the same for $(a, b) = (\uparrow, O)$ and (O, \uparrow) and equals $64\rho^2$ by (3.26b) for our case $\rho \rightarrow 0$. It follows from (B2b) that the \hat{v}^4 -term in the function W in (B3) is of order ρ^4 and can be neglected, since I and $2\hat{v}^2$ are both of order ρ^2 . The integral in (B3) is then trivial and leads to the result (B2b) with the upper sign.

For $b = SB$, the solution follows from (B3) on replacing the lower limit of integration by the positive v -value

$$\left[(1 + |I|)^{1/2} - 1 \right]^{1/2} \quad (\text{B4})$$

for which $W(v)$ vanishes. This guarantees that dv/dr vanishes at $r = R_+$ [61]. For $\rho \rightarrow 0$, in which case $|I| \rightarrow 64\rho^2$ by Eq. (3.26b), one may again neglect \hat{v}^4 inside $W(\hat{v})$, and the lower boundary of integration becomes $(|I|/2)^{1/2}$. The integral is simple and leads to the result (B2b) with the lower sign.

The leading contribution to the energy $\tilde{\Psi} = \Phi^2$ for $d \rightarrow 4$ is given by [62]

$$\langle \Phi^2 \rangle_{\uparrow, b}^{(0)} = \left(\langle \Phi \rangle_{\uparrow, b}^{(0)} \right)^2 \quad (\text{B5})$$

and follows immediately from (B2). Since $\Psi(0) = \Phi^2(0)$, the right hand side of (B1) is, in leading order, the square of its value in the previous cases, and Eq. (B1) is again fulfilled.

Now we turn to the cases where the outer sphere breaks the symmetry, e.g. $b = \uparrow$. For the order-parameter profiles $\tilde{\Psi} = \Phi$ Eq. (B1) implies

$$\langle \Phi(\mathbf{r}) \rangle_{a, \uparrow}^{(0)} \longrightarrow \sqrt{\frac{6}{u}} \frac{v_{\uparrow}^{(\text{fc})}(r) + \delta v_{a, \uparrow}(r)}{r} \quad (\text{B6a})$$

with

$$v_{\uparrow}^{(\text{fc})}(r) = \frac{2\sqrt{2}}{q_-} \quad (\text{B6b})$$

and

$$\delta v_{a,\uparrow}(r) = -\frac{I}{16\sqrt{2}} \left\{ q_- + \frac{12}{q_-} \left[1 - \frac{q_+}{q_-} \ln(\tilde{r}^{-1}) \right] \right\} \quad (\text{B6c})$$

with I from (3.26b) for the four cases $a = (\uparrow, SB, \downarrow, O)$. Here (B6b) represents the non-vanishing profile $\langle \Phi \rangle_{\text{fc}}$ in a full container (fc). It can be obtained by means of a conformal transformation from the half-space profile (3.28) as described e.g. in Ref. [19]. Eq. (B6c) represents the right hand side of (B1). Here $\Psi(0)$ is $(\Phi, \Phi^2, \Phi, \Phi^2)$ in the four cases (see remark just below (3.27)). For $d \rightarrow 4$

$$\langle \Phi(0) \Phi(\mathbf{r}) \rangle_{\text{fc}} - \langle \Phi(0) \rangle_{\text{fc}} \langle \Phi(\mathbf{r}) \rangle_{\text{fc}} \longrightarrow K_{\text{fc}}^{(G)}(r) \quad (\text{B7a})$$

is determined by Gaussian fluctuations φ about the mean-field profile $\langle \Phi \rangle_{\text{fc}}^{(0)}$. The quantity $K_{\text{fc}}^{(G)}$ can be obtained from its counterpart in the half-space whose form is known (see Eq. (4.96) in Ref. [63]). The corresponding correlation for $\Psi(0) = \Phi^2(0)$ follows from

$$\langle \Phi^2(0) \Phi(\mathbf{r}) \rangle_{\text{fc}} - \langle \Phi^2(0) \rangle_{\text{fc}} \langle \Phi(\mathbf{r}) \rangle_{\text{fc}} \longrightarrow 2 \langle \Phi(0) \rangle_{\text{fc}}^{(0)} K_{\text{fc}}^{(G)}(r). \quad (\text{B7b})$$

Note the limits

$$\delta v_{a,\uparrow} \rightarrow -\frac{I}{16\sqrt{2}} \frac{R_+}{r} \quad , \quad r \ll R_+ \quad (\text{B8a})$$

and

$$\delta v_{a,\uparrow} \rightarrow -v_{\uparrow}^{(\text{fc})} \frac{I}{40} \left(\frac{R_+ - r}{R_+} \right)^4 \quad , \quad R_+ - r \ll R_+ \quad (\text{B8b})$$

which follow from Eqs. (B6). Eq. (B8b) is consistent with the expansion (3.33) about the surface, which applies for arbitrary R_-/R_+ .

Again the prediction (B6) of the SSE may be checked by comparing with the solution of the differential equation (3.10a), which is now given by Eq. (3.32). Since v tends to the finite positive value $v_{\uparrow}^{(\text{fc})}$ in (B6b) as $I \rightarrow 0$, one may expand the integrand in (3.32) with respect to I and invert the function $r(v)$ to obtain $v = v(r)$, order by order in I . In first order the result reads

$$v(r) = v_{\uparrow}^{(\text{fc})}(r) \left\{ 1 - \frac{I}{\sqrt{2}} \frac{q_+}{q_-} \int_{v_{\uparrow}^{(\text{fc})}(r)}^{\infty} d\hat{v} [W_0(\hat{v})]^{-3} \right\} \quad (\text{B9})$$

where W_0 is W for $I = 0$. The integral on the right hand side is straightforward, and one sees that Eq. (B9) indeed implies the result (B6).

2. Cases with symmetry preserved in the Gaussian model

Here we consider the $R_- \rightarrow 0$ behavior of the left hand side of (B1) for $\tilde{\Psi} = \Phi^2(\mathbf{r})$ and $a, b \in \{O, SB\}$. The result

$$\left[\langle \vec{\Phi}^2(\mathbf{r}) \rangle_{ab} - \langle \vec{\Phi}^2(\mathbf{r}) \rangle_{fc} \right] / N \longrightarrow \tilde{S}_d \sigma_{ab}^{(2)} (R_-)^{d-2} r^{-2(d-2)} \left[1 + \sigma_{ab}^{(3)} \tilde{r}^{d-2} \right]^2 \quad (B10)$$

follows for the Gaussian model from the $l = 0$ term in (4.23), using $\sigma_{ab}^{(1)} \cdot \sigma_{ab}^{(3)} = \sigma_{ab}^{(2)}$. Note that $\sigma_{ab}^{(2)}$ only depends on a , while $\sigma_{ab}^{(3)}$ only depends on b . This is in agreement with the right hand side of (B1). It is easily verified that (B10) equals the right hand side of (B1): The leading operator is $\Psi = \Phi^2$, and the $\Phi^2 \cdot \Phi^2$ correlation function inside a full spherical container with an O or SB surface, which appears on the right hand side of (B1) in square brackets, follows from its counterpart in the half-space with Dirichlet or Neumann boundary conditions, respectively. The prefactor $A_a^{\Phi^2} / B_{\Phi^2}$ in (B1) is obtained from (3.29) and (3.30).

REFERENCES

- [1] M. E. Fisher and P.-G. de Gennes, *C. R. Acad. Sci. Ser. B* **287**, 207 (1978).
- [2] P.-G. de Gennes, *C. R. Acad. Sci. Ser. B* **292**, 701 (1981).
- [3] For a recent review, see M. Krech, *The Casimir Effect in Critical Systems* (World Scientific, Singapore 1994)
- [4] H. B. G. Casimir, *Proc. K. Ned. Akad. Wet.* **51**, 793 (1948); for a recent review on the Casimir effect in QED, see G. Plunien, B. Müller, and W. Greiner, *Phys. Rep.* **134**, 87 (1986).
- [5] H. W. J. Blöte, J. L. Cardy, and M. P. Nightingale, *Phys. Rev. Lett.* **56**, 742 (1986).
- [6] I. Affleck, *Phys. Rev. Lett.* **56**, 746 (1986).
- [7] J. L. Cardy, *Nucl. Phys. B* **275**, 200 (1986).
- [8] T. W. Burkhardt and T. Xue, *Phys. Rev. Lett.* **66**, 895 (1991); *Nucl. Phys.* **B345**, 653 (1991).
- [9] T. W. Burkhardt and E. Eisenriegler, *Nucl. Phys. B* **424** [FS], 487 (1994).
- [10] K. Symanzik, *Nucl. Phys.* **B190**, [FS3], 1 (1981).
- [11] M. P. Nightingale and J. O. Indekeu, *Phys. Rev. Lett.* **54**, 1824 (1985); J. O. Indekeu, M. P. Nightingale, and W. V. Wang, *Phys. Rev. B* **34**, 330 (1986).
- [12] M. Krech and S. Dietrich, *Phys. Rev. Lett.* **66**, 345 (1991); **67**, 1055 (1991); *Phys. Rev. A* **46**, 1886 (1992); **46**, 1922 (1992).
- [13] E. Eisenriegler and M. Stapper, *Phys. Rev. B* **50**, 10009 (1994).
- [14] T. W. Burkhardt and E. Eisenriegler, to be published.
- [15] D. Beysens and S. Leibler, *J. Physique. Lett.* **43**, L133 (1982); D. Beysens and D. Estève, *Phys. Rev. Lett.* **54**, 2123 (1985); D. Beysens, J.-M. Petit, P. Narayanan, A. Kumar, and M. L. Broide, *Ber. Bunsen Ges. Phys. Chem.* **98**, 382 (1994).
- [16] W. A. Ducker, T. J. Senden, and R. M. Pashley, *Nature* **353**, 239 (1991).
- [17] A. M. Polyakov, *Zh. Eksp. Teor. Fiz. Pis. Red.* **12**, 538 (1970) [Sov. Phys. JETP Lett. **12**, 381 (1970)].
- [18] J. L. Cardy, in *Phase Transitions and Critical Phenomena* Vol 11, Eds. C. Domb and J. L. Lebowitz (Academic Press, London, 1987).
- [19] T. W. Burkhardt and E. Eisenriegler, *J. Phys. A* **18**, L83 (1985).
- [20] Note that the static sphere in electromagnetism or particle physics cannot be discussed in this way. The space-time continuum where there is conformal invariance corresponds to a cylinder and cannot be mapped onto the half-space in $d > 2$.
- [21] S. Gnutzmann and U. Ritschel, *Z. Phys. B*, to be published.

[22] V. Privman and M. E. Fisher, Phys. Rev. B **30**, 322 (1984).

[23] It has been pointed out in J. L. Cardy and I. Peschel, Nucl. Phys. B **300** [FS22], 377 (1988) that $U_a(R)/k_B T_c$ or $\bar{U}_a(R)/k_B T_c$ are, at least in $d = 2$, not scale invariant, i.e. not independent of R , but show a $\log R$ behavior with a universal prefactor; compare also the discussion in V. Privman, Phys. Rev. B **38**, 9261 (1988) for systems in $d > 2$. According to Cardy and Peschel the reason is that the average of the trace of the stress tensor has at the critical fixed point a non-vanishing delta-function contribution on the curved boundary of the critical medium. The prefactor of this contribution is given by the local curvature of the boundary ($\pm R^{-d+1}$ for the spherical boundary) times a number which depends only on the universality class of the bulk and, for $d > 2$, possibly of the surface. Thus the delta-function contribution from the surface of the a -particle, say, is independent of the presence of the b -particle and cancels for the difference of stress-tensor trace averages, which when multiplied with the local dilatation and integrated over space determines the change of δF in (1.7) under an infinitesimal conformal transformation; compare Ref. [18] and Eq. A3 below. The conformal invariance of δF in (1.7) will be explicitly verified in Appendix A (see the paragraph containing Eq. (A7)) by using the transformation formula (2.18a) for the stress tensor at interior points and transforming to the concentric geometry.

[24] K. G. Wilson and J. Kogut, Phys. Rep. **12**, 75 (1974).

[25] K. Binder, in *Phase Transitions and Critical Phenomena* Vol 8, Eds. C. Domb and J. L. Lebowitz (Academic Press, London, 1983).

[26] H. W. Diehl, in *Phase Transitions and Critical Phenomena* Vol 10, Eds. C. Domb and J. L. Lebowitz (Academic Press, London, 1986)

[27] T. W. Burkhardt and J. L. Cardy, J. Phys. A **20**, L233 (1987).

[28] T. W. Burkhardt and H. W. Diehl, Phys. Rev. B **50**, 3894 (1994).

[29] V. Dohm, Physica Scripta T **49**, 46 (1993).

[30] J. L. Cardy, Phys. Rev. Lett. **65**, 1443 (1990)

[31] E. Eisenriegler, M. Krech, and S. Dietrich, Phys. Rev. Lett. **70**, 619 (1993) and to be published; M. Krech, E. Eisenriegler, and S. Dietrich, to be published.

[32] In many respects a boundary acts qualitatively like an assembly of operators.

[33] Here the tilde serves to distinguish the primary operators $\tilde{\Psi}$ from those which appear in the sum (2.6b). The latter (which are special Ξ 's) are denoted by Ψ , compare Eq. (2.10) below. Both $\tilde{\Psi}$ and Ψ may be either the order parameter or the energy density.

[34] An expansion of the form (2.6) will also exist if the ‘small object’ is not a sphere but, for example, a *cube* with edge length R_S . While the leading operators Ξ in σ should be the same as for the sphere, the prefactors \mathcal{X} will not, in general, be expressible in terms of half-space amplitudes. We expect additional operators which reflect the anisotropy of the cube. For an infinite *cylinder* or ‘wire’ with diameter $2R$ (or a hyperprism with $d-1$ finite equilateral edges and one edge of infinite extent), we expect an expansion of the

form (2.6), the leading Ξ being a line integral $\int_{-\infty}^{\infty} dt \Psi(\mathbf{e} t)$ with the unit vector \mathbf{e} in the infinite direction and with prefactor $\mathcal{X} \sim R^{x_\Psi-1}$. Here we consider cases where $x_\Psi - 1$ is positive and the line integral is an ‘irrelevant’ bulk perturbation (compare A. Bray and M. A. Moore, J. Phys. **A** 10, 1927 (1977), and T. W. Burkhardt and E. Eisenriegler, Phys. Rev. **B** 24, 1236 (1981) for a corresponding discussion of defect planes). The expansion has been checked for the simple case of the order parameter correlation in an infinite Gaussian model with a cylindrical hole with Dirichlet boundary conditions in $d > 3$. (For $d < 3$ the long-distance decay of the correlation along the cylinder is governed by an exponent larger than the bulk exponent $d - 2$, and the expansion does not apply.) In this case $\Psi = \Phi^2$, and the amplitude $\mathcal{X}/R^{x_\Phi-1} = \mathcal{C}(d)$ can be explicitly determined. For the interaction free energy δF_{12} of *two crossed wires* with O (ordinary) boundary conditions, diameters $2R_1, 2R_2$, and a minimal separation $s_{12} \gg R_1, R_2$, one finds $\delta F_{12} = -k_B T_c (R_1 R_2 / s_{12}^2)^E \mathcal{C}^2 \mathcal{D}$ from the arguments which led to Eq. (15) in Ref. [14]. Here $E = x_\Phi - 1 = d - 1 - 1/\nu = 0.51$ for $d = 3$, $N = 2$, which should apply to ${}^4\text{He}$. The quantity $\mathcal{D} = \int_{-\infty}^{\infty} dt_1 dt_2 \langle \Phi^2(\mathbf{e} t_1) \Phi^2(\mathbf{s}_{12} + \mathbf{e} t_2) \rangle_{\text{bulk}} \cdot s_{12}^{2E}$ is independent of s_{12} but depends on the angle between the wires.

[35] For simplicity consider $T > T_c$. Both the finite bulk correlation length $\xi \sim (T - T_c)^{-\nu}$ and the ‘large’ distances mentioned right after Eq. (2.6b) have to be much larger than R_S in order that Eqs. (2.6) apply. The amplitudes \mathcal{X}_Ψ are independent of $T - T_c$ and are given by (2.10) as before. Since the bulk average of σ is for $T > T_c$ in general non-vanishing, one obtains slightly different relations. For example the right hand side of (2.7) has to be supplemented by subtracting the product $\langle \sigma \rangle_{\text{bulk}} \cdot \langle \tilde{\Psi}(\mathbf{r}) \rangle_{\text{bulk}}$. This may e.g. be verified for the simple case when $\tilde{\Psi}(\mathbf{r})$ is the energy density around a single spherical hole with an ordinary (O) surface in an infinite Gaussian model at $T > T_c$. Then the left hand side of (2.7) can for arbitrary ratios $R_S/r, R_S/\xi$ be represented by a sum over angular momentum numbers (similar to Eqs. (4.2) or (4.14)); compare E. Eisenriegler, Z. Phys. B **61**, 299 (1985). For two distant spheres at $T > T_c$ with $R_1, R_2 \ll \xi, s_{12}$, Eq. (2.6a) implies that δF defined in (1.7) is $-k_B T \ln [\langle (1 + \sigma_1)(1 + \sigma_2) \rangle_{\text{bulk}} / (\langle 1 + \sigma_1 \rangle_{\text{bulk}} \langle 1 + \sigma_2 \rangle_{\text{bulk}})]$ in an obvious notation. Using (2.10), the leading behavior of δF is given by the right hand side of (2.15a) with $s_{12}^{-2x_\Psi}$ replaced by the normalized bulk correlation function $[\langle \Psi(1)\Psi(2) \rangle_{\text{bulk}} - \langle \Psi \rangle_{\text{bulk}}^2] / B_\Psi$ at $T > T_c$, where the two points 1, 2 are separated by the distance s_{12} . For the sphere in a half space (SPW geometry) at $T > T_c$ with $R_1 \ll \xi, D$, the interaction energy δF_{SPW} can be written like the left hand side of (2.8); only the full container fc in (2.8) has to be replaced by the half space. Eqs. (2.6) imply for δF_{SPW} a leading behavior given by the right hand side of (2.15b) with the half-space profile $A_b^\Psi (2D)^{-x_\Psi}$ at $T = T_c$ replaced by the difference $\langle \Psi(\mathbf{r}_\parallel, D) \rangle_{\text{half space}} - \langle \Psi \rangle_{\text{bulk}}$ of the profile at $T > T_c$ and its bulk limit.

[36] In the Landau–Ginzburg model the energy density operator $\mathcal{E}(\mathbf{r})$ is proportional to $-\vec{\Phi}^2(\mathbf{r})$ on account of the thermodynamic bulk relation $\langle \mathcal{E} \rangle_{\text{bulk}} / k_B T = -T \frac{d f_{\text{bulk}}}{dT} \sim -\langle \vec{\Phi}^2 \rangle_{\text{bulk}}$ with f_{bulk} the corresponding free energy density. Since we use dimensional regularization [45], the bulk average of $\vec{\Phi}^2$ vanishes at T_c . For the universal amplitude ratios considered below, the (negative) factor between \mathcal{E} and $\vec{\Phi}^2$ does not matter, and we refer to $\vec{\Phi}^2$ as the energy density.

[37] We denote the normal–normal component of the stress tensor by T_{nn} in the concentric geometry of Fig. 1 a, where the normal is in the radial direction and by $T_{\perp\perp}$ in geometries of the type depicted in Fig. 1 b, where the normal is on curved lines which are perpendicular to all the spherical \mathbf{r}' -images of concentric \mathbf{r} -spheres. In particular the lines are perpendicular to the plane $r'_\perp = 0$.

[38] Here we consider situations where both the bulk and the two surfaces are at critical fixed points of the renormalization group. It is only in this case that dilatation and conformal invariance hold on all length scales.

[39] D. M. McAvity and H. Osborne, Nucl. Phys. B **406**, 655 (1993).

[40] For our two-sphere geometries, it follows from (2.3) by means of the conformal transformation (1.1) which itself is regular near the boundaries.

[41] In $d = 2$, $C_\Psi^{(b)} = 4\pi x_\Psi/c$ is hyperuniversal, i.e. independent of b [8]. Here c is the bulk conformal charge of the two-dimensional system, see A. A. Belavin, A. M. Polyakov, and A. B. Zamolodchikov, J. Stat. Phys. **34**, 763 (1984) or Ref. [18].

[42] Below we consider the Gaussian model ($u = 0$) for arbitrary spatial dimension $d > 2$ and the Φ^4 -model in dimensional regularization and within the ϵ -expansion. In both cases there is no Φ^2 term in \mathcal{L} at the bulk critical point.

[43] C. Callan, S. Coleman, and R. Jackiw, Ann. Phys. (NY) **59**, 42 (1970).

[44] L. S. Brown, Ann. Phys. (NY) **126**, 135 (1980).

[45] D. J. Amit, *Field Theory, the Renormalization Group and Critical Phenomena*, (McGraw-Hill, New York, 1978).

[46] J. Zinn-Justin, *Quantum Field Theory and Critical Phenomena*, (Clarendon Press, Oxford, 1989).

[47] P. G. Leach, J. Math. Phys. **26**, 2510 (1985).

[48] W. Sarlet and L. J. Bahar, Int. J. Non-Linear Mech. **15**, 133 (1980).

[49] dv/dr vanishes, however, at the SB surface (cf. Ref. [21]).

[50] D. M. McAvity and H. Osborne, Nucl. Phys. B **394**, 728 (1993).

[51] Here the integrand on the right hand side of (3.32) is integrated from zero, the value of v at the O -surface, to v . Close to the O -surface v is small, and the integrand can be expanded in powers of \hat{v} .

[52] Apart from being the simplest example for a family of d -dependent conformal theories, the model describes tricritical behavior for $d \geq 3$, apart from possible logarithmic corrections in $d = 3$.

[53] M. Abramowitz and I.A. Stegun, *Handbook of Mathematical Functions*, (Dover Publications, New York, 1972).

[54] I. S. Gradshteyn and I. M. Ryzhik, *Table of Integrals, Series, and Products*, (Academic

Press, New York, 1980).

- [55] While the complete functions \mathcal{F} have only been obtained to leading order in the ϵ -expansion, most of the universal amplitudes that determine the limiting behaviors are available to leading and next-to-leading order. Corresponding results for the amplitude in (2.15a) for $\kappa \rightarrow \infty$ can be inferred from [13] and [31] and are shown in Eqs. (20), (21) of [14]. The amplitudes in (2.5) for $\kappa \rightarrow 1$ in the symmetry-preserving cases follow from Ref. [12].
- [56] J. C. Le Guillou and J. Zinn-Justin, *J. Physique Lett. (Paris)* **46**, L137 (1985).
- [57] R. J. Hunter, *Foundations of Colloid Science*, (Oxford, Clarendon 1989).
- [58] J. C. Crocker and D. G. Grier, *Phys. Rev. Lett.* **73**, 352 (1994).
- [59] If the separation is not much larger than the radius, multiparticle interactions appear, which can be related to multispin correlation functions in the Ising model [14].
- [60] Note that at $T = T_c$ ($\xi = \infty$) the total potential energy is more than extensive: For a quasi-close-packed configuration of \mathcal{N} aggregated colloid particles, from (5.1) the potential energy per particle is $\sim -\mathcal{N}^{1-F/d} = -\mathcal{N}^{0.65}$. Here F is the exponent 1.04 in the pair potential (5.1) and $d = 3$ the space dimension. Contrary to the usual thermodynamic behavior (which applies for $F > d$), the energy per particle increases with particle number, and the prefactor depends on the shape of the aggregate. For long-distance pair attraction $\sim s^{-F}$ with $F < d$ the statistical mechanics appears to be quite interesting and unusual. For a discussion of gravitational interactions ($F = 1$, $d = 3$), see K. H. Kiessling, *J. Stat. Phys.* **55**, 203 (1989) and references therein.
- [61] See discussion of the solutions for (\uparrow, SB) below (3.17).
- [62] $\langle \Phi^2 \rangle_{fc,b}$ is non-vanishing for $b = O$ or SB , but does not contain a contribution of order $1/u$.
- [63] D. Jasnow, in *Phase Transitions and Critical Phenomena* Vol 11, Eds. C. Domb and J. L. Lebowitz (Academic Press, London, 1987)

Figure Captions

Fig. 1: Conformal mapping of concentric spheres with center at the origin of \mathbf{r} -space (Fig. 1 a) onto spheres in \mathbf{r}' -space with centers on the line $\mathbf{r}' = r'_\perp \mathbf{R}/R$ (Fig. 1 b) as implied by Eq. (1.1). The sphere denoted by the broken line with radius R is mapped onto the plane $r'_\perp = 0$. The two points $\mathbf{r} = -\mathbf{R}$ and $\mathbf{r} = \mathbf{R}$ of this sphere are mapped onto $\mathbf{r}' = 0$ and $\mathbf{r}' = \infty$, respectively. The two spheres with radii R_- and R_+ are mapped on spheres with radii R_1 and R_2 , respectively. The corresponding intersection points of the two spheres with the coordinate axes parallel \mathbf{R} are denoted by I, II, III, IV. For the case $R_- < R < R_+$ shown in Fig. 1 a the images $\mathbf{r}' = 2\mathbf{R}$ and $\mathbf{r}' = -2\mathbf{R}$ of $\mathbf{r} = 0$ and $\mathbf{r} = \infty$ are located inside the two spheres in Fig. 1 b and are closer to the origin than the centers of the spheres.

Fig. 2: Scaling functions $\mathcal{F} = \mathcal{F}_{ab}$ in a critical Ising-type ($N = 1$) system for spatial dimension $d \rightarrow 4$. The function \mathcal{F}_{OSB} , which is not shown, would nearly coincide with $-\mathcal{F}_{OO} = -\mathcal{F}_{SB\,SB}$ in this plot. For the four symmetry-breaking combinations $(a\,b) = (\uparrow\downarrow)$, $(\uparrow\uparrow)$, $(\uparrow\,O)$, $(\uparrow\,SB)$, the functions \mathcal{F} behave as $1/\epsilon$ for $d \rightarrow 4$, and we have plotted the finite limit $\tilde{\mathcal{F}}_{ab} = \lim_{d \rightarrow 4} (4 - d) \mathcal{F}_{ab}$.

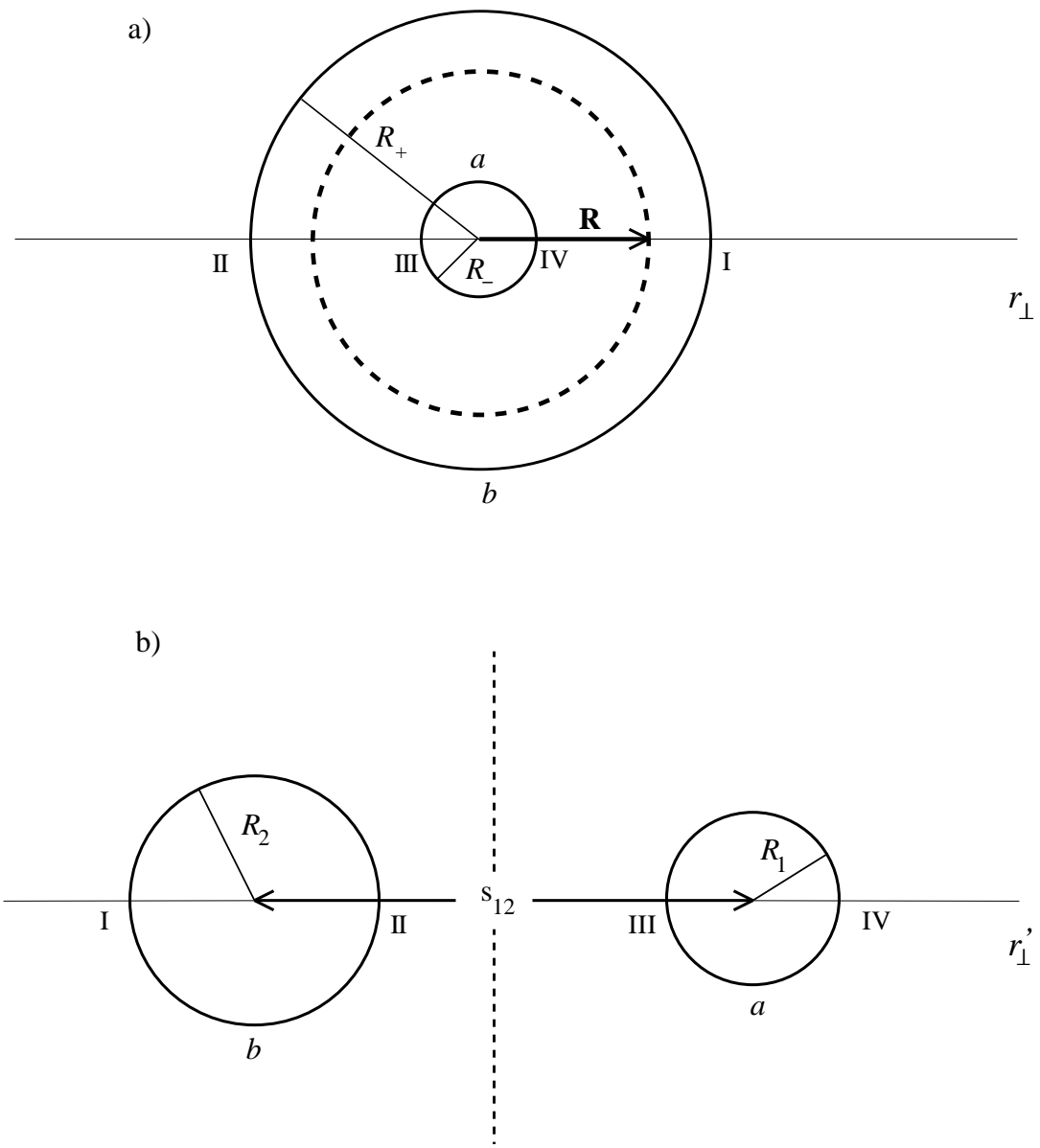


Fig. 1

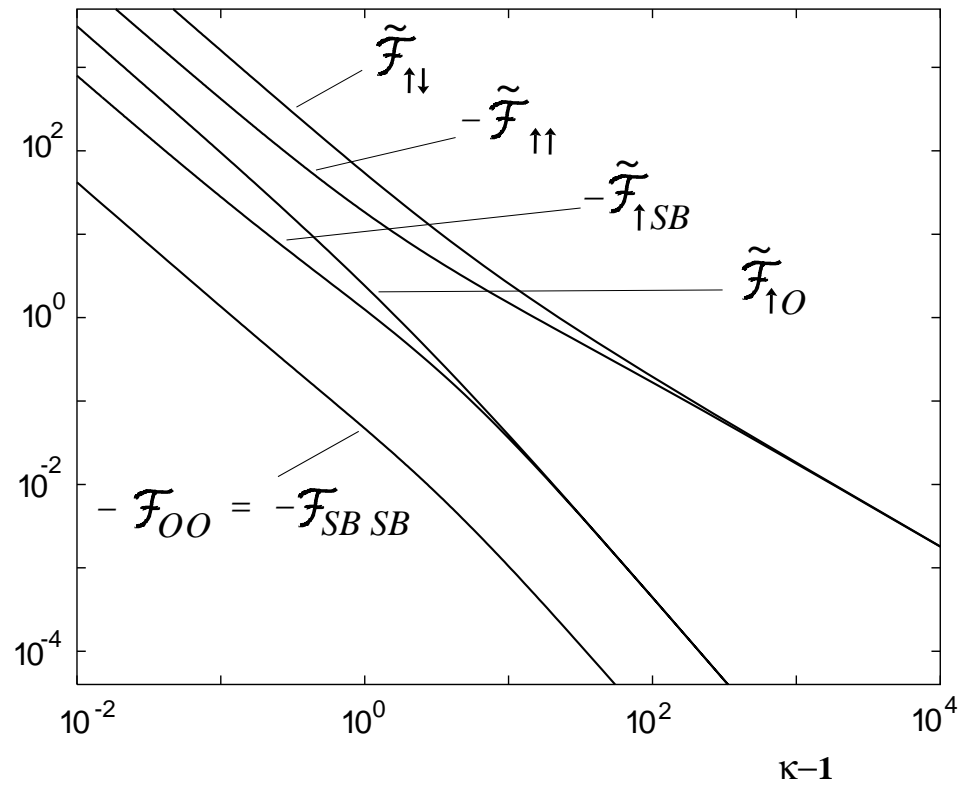


Fig. 2